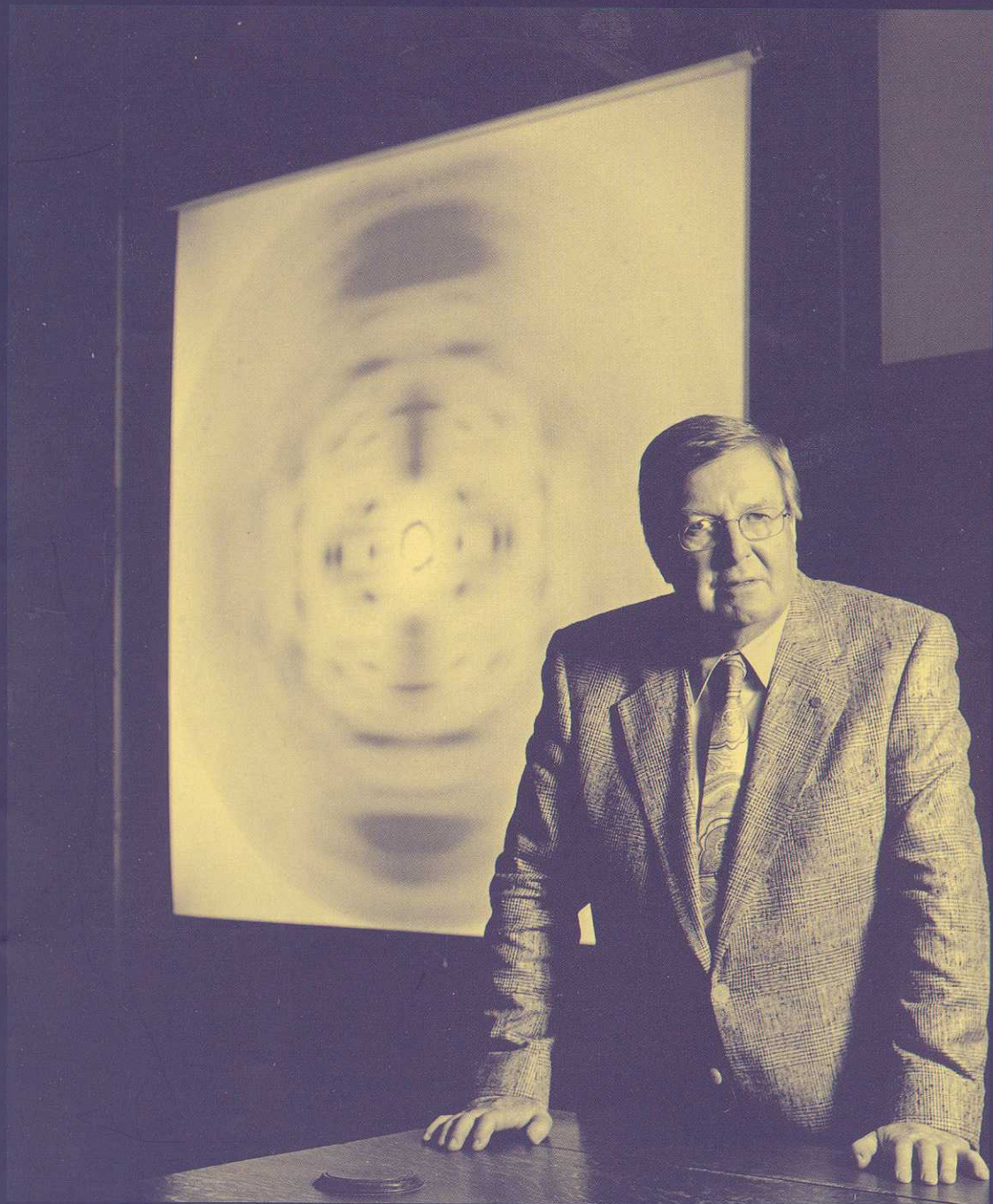


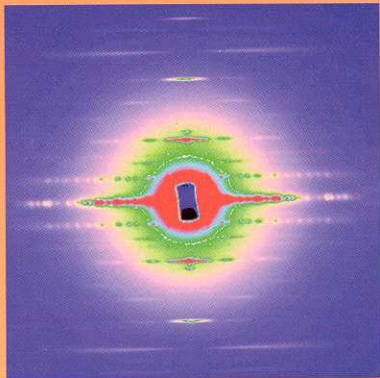
# FIBRE DIFFRACTION REVIEW

**THE CCP13 NEWSLETTER**  
*Software Development for Fibre Diffraction*

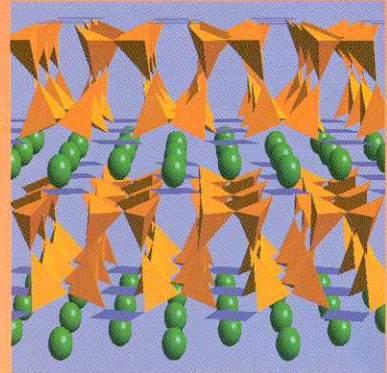


Issue 8

December 1999



# DARTS



## The Daresbury Synchrotron Radiation Service

**Access to the unique properties of synchrotron radiation with a range of techniques**

**Rapid access and sample turn-round**

**Free for academic customers**

**Complete commercial confidentiality**

**Accelerated delivery of results**

**Service tailored to match your requirements**

**Support facilities available**

**DARTS Manager**  
Daresbury Laboratory  
Warrington WA4 4AD, UK

phone +44 (0)1925 603141  
FAX +44 (0)1925 603124  
e-mail darts@dl.ac.uk

<http://www.srs.dl.ac.uk/DARTS>



Daresbury Analytical Research and Technology Service

# Contents

Contents, Cover Caption and Production .....	1
The CCP13 Committee Members .....	2
Chairman's Message .....	3

## Meeting Reports

CanSAS II, T. Irving .....	4
SAS99, XIth International Conference on Small Angle Scattering, N. Terrill .....	5
CCP13 and NCD Training Workshop, M.W. Shotton .....	6
Denver X-ray Conference, J.P.A. Fairclough .....	7
8th Annual CCP13 Workshop, R.C. Denny .....	8

## Technical Developments

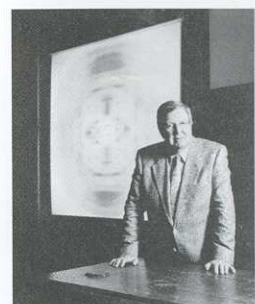
Beamline 14 and the Opportunities for Fibre Diffraction, E.M.H. Duke .....	11
POLO Detector: 5 CCD SAXS/WAXS area detector for Synchrotron Radiation, J.P.A. Fairclough <i>et al.</i> ..	12
CCP13 Software Development, M.W. Shotton <i>et al.</i> .....	14
Summary of Available CCP13/NCD Software .....	20

## Contributed Articles

Lessons for Today and Tomorrow from Yesterday, S. Arnott .....	21
X-Ray Studies on Biological Fibres, A. Miller <i>et al.</i> .....	27
Unravelling Starch Granule Structure with Small Angle Scattering, A.M. Donald <i>et al.</i> .....	31
Structure of Block Copolymer Solutions, T. P. Lodge <i>et al.</i> .....	37
The Crystal Structure and Hydrogen Bonding System in Cellulose from Neutron Fibre Diffraction Data, P. Langan <i>et al.</i> .....	42
Chromatin Higher-Order Structure: Results from Small-Angle X-Ray Scattering and Histone-Octamer Crystallography, J. Kilner <i>et al.</i> .....	48
Real time FTIR and WAXS studies of the drawing behaviour of polyethylene terephthalate fibres, A.C. Middleton <i>et al.</i> .....	53

## 8th Annual Workshop Prize-Winning Posters

An XRD Study of the Rigid-Rod Polymer Fibre M5 (PIPD), E.A. Klop <i>et al.</i> .....	58
X-Ray Analysis of the network-forming collagen in the Dogfish <i>Scyliorhinus Canicula</i> Egg Case, C. Knupp <i>et al.</i> .....	61
8th Annual Workshop Abstracts .....	67
Forthcoming Meetings .....	79
<i>Fibre Diffraction Review: Instructions to Authors</i> .....	80



## Front Cover Image

Struther Arnott with an X-ray fibre pattern of poly d(GC).poly d(GC) in its rarer Z-form. The photograph is part of a triptych by Robin Gillanders commissioned by the Myers' Trusts to celebrate Struther Arnott's 1986-2000 tenure as Principal/Vice-Chancellor/Scientist at St. Andrews.

## Newsletter Production

**Editor:** Prof. J. Squire, Biological Structure and Function Section, Biomedical Sciences Division, Imperial College, London SW7 2AZ.

**Production:** Dr M.W. Shotton, Dr R. Denny and Dr G. Mant, Daresbury Laboratory, Warrington WA4 4AD.

**Printer:** Eaton Press Ltd, Westfield Road, Wallasey, Merseyside L44 7JB. (Tel. 0151-652 9111, Fax 0151-653 5936)

# The CCP13 Committee Members (1998)

**Chairman** Dr Trevor Forsyth (to 2002)

Institut Laue-Langevin, BP 156 F-38042, Grenoble Cedex 9, France, and Physics Dept, Keele University, Staffordshire ST5 5BG

**Phone** +33 4 (0) 76207158 **Fax** +33 4 (0) 76483906 **Email** tforsyth@ill.fr

**Secretary** Dr Richard Denny (to 2001)

Daresbury Laboratory, Daresbury, Warrington WA4 4AD

**Phone** 01925 603169 **Email** r.denny@dl.ac.uk

**Research Assistant (Ex Officio)** Dr Mark Shotton

Daresbury Laboratory, Daresbury, Warrington WA4 4AD

**Phone** 01925 603626 **Email** m.shotton@dl.ac.uk

## Members

Dr David Blundell (to 2002)

Physics Department, Keele University, Keele, Staffordshire, ST5 5BG

**Phone** 01782 583330

Dr Patrick Fairclough (to 2002)

Department of Chemistry, The University of Sheffield, Dainton Building, Brookhill, Sheffield, S3 7HF

**Phone** 0114 2229411 **Fax** 0114 2229303 **Email** p.fairclough@sheffield.ac.uk

Dr Mike Ferenczi (to 2001)

National Institute for Medical Research, Ridgeway, Mill Hill, London NW7 1AA

**Phone** 0181 959 3666 **Email** m.ferenc@nimr.mrc.ac.uk

Dr Steve King (to 2001)

Rutherford Appleton Laboratory, Chilton, Didcot, OX11 0QX

**Phone** 01235 446437 **Fax** 01235 445720 **Email** s.m.king@rl.ac.uk

Prof. John Squire (to 2002)

Biomedical Sciences Division, Imperial College, London SW7 2AZ

**Phone** 0207 594 3185 **Fax** 0207 594 3169 **Email** j.squire@ic.ac.uk

Dr Tim Wess (to 2002)

Department of Biological and Molecular Sciences, University of Stirling, Stirling, FK9 4LA

**Phone** 01786 467775 **Fax** 01786 464994 **Email** tzw3@stir.ac.uk

## Members (Co-opted)

Dr Greg Diakun

Daresbury Laboratory, Daresbury, Warrington WA4 4AD

**Phone** 01925 603343 **Email** g.diakun@dl.ac.uk

Dr Tom Irving

CSRRI, Dept BCPS, Illinois Institute of Technology, 3101 s. Dearborn, Chicago IL. 60616, USA

**Phone** (312) 567-3489 **Fax** (312) 567-3494 **Email** irving@biocat1.iit.edu

Dr Rob Lewis

Daresbury Laboratory, Daresbury, Warrington WA4 4AD

**Phone** 01925 603544 **Email** r.a.lewis@dl.ac.uk

Dr Geoff Mant

Daresbury Laboratory, Daresbury, Warrington WA4 4AD

**Phone** 01925 603169 **Email** g.r.mant@dl.ac.uk

Prof. Rick Millane

Whistler Center, Purdue University, West Lafayette, Indiana 47907-1160 USA

**Phone** (765) 494-9272 **Email** rmillane@purdue.edu

Dr Keiichi Namba

Matsushita Electric Industrial Co. Ltd., 3-4 Hikaridai, Seika 619-0237, Japan

**Phone** 81-774-98-2543 **Fax** 81-774-98-2575 **Email** keiichi@crl.mei.co.jp

Prof. Gerald Stubbs

Dept of Molecular Biology, Vanderbilt University, 2200 West End Avenue, Nashville, TN 37235

**Phone** (615) 322-7311 **Email** stubbs@ctrvax.vanderbilt.edu

## Chairman's Message

For all sorts of reasons, last year was something of a turning point for CCP13. John Squire, after forming CCP13 as an SERC initiative some eight years ago, stepped down as Chairman. In his wake he leaves a software initiative that has established an excellent international reputation as a development node for fibre diffraction and non-crystalline diffraction software. It is also one that has had a very clear impact on many biological and non-biological problems. While it is true that CCP13 owes its success to many people, the simple truth is that without John Squire, it would not even exist. We are lucky that John is going to stay heavily involved with CCP13; he remains on the steering committee and also as the editor of *Fibre Diffraction Review*, the CCP13 newsletter that has essentially grown out of its boots and has recently become a refereed journal.

I think that it is also significant that within the last year or so, the full impact of CCP13 activity has started to sink into the wider scientific community. There has always been a large user community in the fibre diffraction/non-crystalline diffraction area. One of the goals of CCP13 was to eliminate the huge duplication of effort that was going on with software and to produce a suite that interfaced well at all levels and indeed where appropriate to other software packages (e.g. CCP4). Predictably, the UK community latched on to what was happening with CCP13 quickly, but it is only rather more recently that its impact at an international level has become apparent. Indeed it is gratifying to see CCP13 being reviewed so favourably in mainstream journals such as *Current Opinion in Structural Biology*. With the benefit of hindsight (always nice), it seems easy to see how it has all come together so well:

Firstly, the CCP13 package itself has been extremely well conceived and constructed, mainly as a result of exceptional efforts by Richard Denny, Geoff Mant, and now Mark Shotton. It offers flexible programs that can be applied to a wide range of problems and that are backed with full mathematical rigour. Where appropriate, clear, uncomplicated graphical user interfaces (GUIs) facilitate the use of these programs, making life considerably easier for new users. It is a tribute to the people involved that the CCP13 initiative is, I believe, also on the right track technically. All GUIs are now written in Java and there has been careful evaluation of the relative merits of procedural and object oriented

programming for different types of application. In short, CCP13 has its finger on the pulse!

Secondly, to the credit of the steering committee, the project has always had a strong sense of direction. While originally aimed at biological problems involving filamentous molecules (e.g. DNA, filamentous viruses, muscle, collagen, cellulose etc.), a decision was made at an early stage to ensure that the software was sufficiently general to apply to non-biological systems and also to disordered polymers and solutions. This is highlighted by the fact that what started off as a purely SERC (biology) and then BBSRC funded activity is now jointly funded by the BBSRC and Daresbury Laboratory, reflecting approximately 50% activity in biological and non-biological areas.

Thirdly, CCP13, together with the Non Crystalline Diffraction (NCD) group at Daresbury, has always attached great importance to the workshops it organises each year, both in terms of the quality of the programme and of the 'hands on' training sessions that have become such a useful feature of the workshop. The first seven of these workshops were held at Daresbury Laboratory but as interest in the project has developed, the possibility of holding these workshops elsewhere arose. Last year the annual workshop was held at St. Andrews University, in honour of Struther Arnott, who has made pivotal contributions to the field of fibre diffraction. By general agreement, the meeting was the best we have ever had and I hope we can continue this trend with the forthcoming meeting at Sheffield University in June 2000.

Lastly, looking through previous copies of the newsletter, I am struck by the steady evolution in the quality of the document and the articles it contains. It started off, as planned, as an informative pamphlet containing useful and relevant information for CCP13 activity. It now exists as a refereed journal, *Fibre Diffraction Review* (ISSN 1463-8401), that in addition to core CCP13/NCD information, contains papers presented at the annual workshop as well as contributed articles. Much of this change is due to the efforts of Geoff Mant and Richard Denny, who have worked very hard on the presentation of the journal. John Squire, as editor, has also over the years consistently pushed the quality of the publication. However, it goes without saying that in

the end, the journal is nothing without your contribution as users. Please remember this for future issues – this is *your* journal and its success will help to ensure continued support of CCP13 from the BBSRC and from Daresbury Laboratory. Whether you are an industrialist, academic staff, or a postgraduate student, please consider submitting articles or reviews of your work to *Fibre Diffraction Review*. We cannot guarantee publication but I know that John will make sure that all articles are refereed well. If it is published, your article will land on the desks of just about everybody in the field.

Please *do* come to the Sheffield meeting in June and please *do* submit your work (whether as a review or otherwise) to *Fibre Diffraction Review*. Please also remember that in addition to the training sessions held at the main annual meeting, CCP13/NCD now runs separate software training workshops for newcomers to the software. Last year the first of these was held at Daresbury Laboratory and was

organised by Mark Shotton and Nick Terrill. About 17 people attended and the feedback was very positive. The timing and location of this training workshop makes it an ideal and cheap way for new students to familiarise themselves with the field. If you require any further information on CCP13 and NCD, remember the website at <http://www.dl.ac.uk/SRS/CCP13>. Also take the few minutes or so that are needed to subscribe to the CCP13 bulletin board (instructions for this at the website).

It just remains for me to thank all those involved for their efforts over the years and to welcome our new steering committee members, Keiichi Namba (Japan), Tom Irving (Illinois, USA), Gerald Stubbs (Vanderbilt, USA), and Rick Millane (Purdue, USA). We are delighted to have their input on the panel.

Trevor Forsyth

Institut Laue Langevin and Physics Department,  
Keele University

## Meeting Reports

### CanSAS II, 16th May 1999, Brookhaven National Laboratory

On May 16th 1999, a workshop entitled “Data Handling for Small-Angle Scattering” a.k.a. “canSAS II” was held at Brookhaven National Labs as a prelude to the worldwide SAS 99 Congress. The workshop was chaired by John Barnes of NIST, (the chair of the IUCr Commission on Small-Angle Scattering who sponsored the workshop). “canSAS” stands for “Collective Aid to Nomadic Small-Angle Scatterers.” “canSAS I” was a workshop in Grenoble in February of 1998 attended mainly by “Instrument Responsibles”. canSAS II, in contrast, represented an attempt to bring data handling issues to the larger SAS community which was represented by about 90 attendees.

Wim Bras kicked off the workshop with an overview of the accomplishments of canSAS I and some of the issues raised at the time. More general talks were “Using Statistics to Assess SAS Data Quality” by John Barnes, “Resolution Issues in SAS” by John Barker also of NIST, and “Modeling and Goodness of Fit in SAS Data Reduction” by Jan Skov Pedersen, Risoe. The remainder of the talks and the subsequent panel discussion were aimed directly at

the concerns brought out in canSAS I, namely how can we make it easier for users to take home their data and interpret it once they get there? To this end Marc Malfois and Dmitri Svergun from EMBL, Hamburg talked about “sasCIF - A Proposed Standard for 1-D SAS”. Joachim Kohlbrecher, PSI, followed up with “One User’s Experience with Nexus” which dealt with the Nexus file format, a work in progress which proposes a standard file format for arbitrary SAS data based on HDF. Richard Heenan, of ISIS, followed up with “Existing Tools for SAS Nomads” which was a comprehensive overview of existing programs and their availability.

The remainder of the workshop consisted of a panel discussion moderated by myself (Tom Irving, BioCAT). The main issues that were discussed were:

- 1) How to make it easier for users to get access to their data.
- 2) Are we in a position to bless a “standard format” or formats?
- 3) Can we move towards a “gold standard” software package or packages?

The sasCIF ASCII format allows simple text tools to get at data. Although no-one could claim that there were any definitive answers to any of these questions, it was clear that there were some positive movements in that direction, however glacial.

Clearly portable, widely supported, self-describing file formats would assist users greatly with using data from a variety of facilities. There is still controversy whether the best approach is to develop and widely distribute routines for converting the formats used into one or more “standard formats” once they have been determined or to rewrite existing code to use the new formats? The advantage of the former is that it is less work for the programmers. In the discussions both sasCIF and Nexus appear to be viable candidates for “standard formats”. ImageCIF (for 2-D) and sasCIF could fit naturally together and would be likely to get the stamp of approval from IUCr. It was resolved that new facilities should be encouraged to support one or both of sasCIF and Nexus and see which meets the needs best, as well as giving feedback data for the developers. Tom Irving, BioCAT, and Wim Bras, Dubble CRG, said they would endeavor to do so.

Can we move towards a “gold standard” software

package or packages? It was recognized that currently available packages are hard to find and documentation varies widely in adequacy still, despite many efforts by various people to improve this situation. The basic problem is that these outreach activities are generally too time-consuming for busy developers to support. The group was informed that the CCP13 project had recently taken SAS as part of its purview. It was suggested that Mark Shotton (the main CCP13 maintainer) should be invited to visit various facilities with established code bases to get a handle on the magnitude of the problem and see what can be done. People who would like to help in this way should contact Mark at m.shotton@dl.ac.uk. The workshop ended with a discussion of future canSAS meetings. There seemed to be a consensus that a “technical” canSAS meeting should be scheduled in 18 months or so. The next international SAS meeting in 2002 would be the next opportunity to communicate progress with the larger community of users.

Tom Irving  
Associate Director BioCAT  
CSRRI, Dept. BCPS, Illinois Institute of Technology  
3101 S. Dearborn, Chicago IL. 60616, USA  
(312) 567-3489 FAX: (312)567-3494

## SAS99, XIth International Conference on Small Angle Scattering, 17th-20th May 1999, Brookhaven National Laboratory

The XIth International Conference on Small Angle Scattering was held at the Brookhaven National Laboratory (BNL) on Long Island, New York in the USA. BNL was founded in 1947 on the site of the U.S. Army's former Camp Upton, by a non-profit educational consortium called Associated Universities, Inc. under contract to the Atomic Energy Agency. Brookhaven Science Associates now operate BNL for DOE, they are a partnership of the State University of New York at Stony Brook and the Battelle Memorial Institute.

The Brookhaven facility carries out basic and applied research in physical, biomedical and environmental sciences together with energy based technologies at its various centres of excellence. These include an Accelerator Test facility for High Energy Physics and accelerator research, an Alternating Gradient Synchrotron to provide protons for High Energy Physics, a High Flux Beam Reactor for neutron

experiments and The National Synchrotron Light Source with X-ray and vacuum ultra violet rings. They are in the process of commissioning RHIC, a Relativistic Heavy Ion Collider with a 3.8km diameter ring, used in the study of atomic particles.

With a meeting of this size it would be impossible to give justice to all the topics that were up for discussion so instead what follows are a few of the highlights.

One of the features of the meeting was the excellent work now being carried out at a number of third generation sources in the field of microfocus X-ray scattering. In particular Christian Riekel gave an excellent presentation on the recent advances in microfocus work carried out at the ESRF on beamline ID13. These included new developments in the field of microfocus collimation *e.g.* capillaries, mirrors and waveguides which can give useful X-ray

beams down to 2µm, small enough to examine cellulose microfibrils in native flax. There was also an interesting presentation on Fruit Fly muscle by Tom Irving using his beamline at the APS in microfocus configuration. Dmitri Svergun presented some very interesting analysis on solution scattering work carried out at the ESRF utilising newly developed software. Veronica James, who spoke about her work on using hair as a marker for breast cancer and insulin dependent diabetes, presented the most radical lecture of the meeting. A lively discussion was held after the presentation on the merit of the work, which included contributions from the floor of the meeting from others that study the subject.

On the Wednesday of the meeting the plenary session was given over to a tribute to Paul W. Schmidt with

contributions given by colleagues and friends during his distinguished career. Prof. John Squire gave a “virtuoso” performance giving the conference lecture. “Movements in a Molecular Symphony - Diffraction Probing of Nature’s Linear Motor” was a very enjoyable combination of science and music. The classical music was an agreeable addition to the 3-D images, which made understanding the structural complexities of muscle much easier.

The final news item from the conference is the contest for the location of the next SAS meeting. In a “not-so-close” contest with the ESRF, the Italian party from TRIESTE won the right to host the next SAS meeting in Venice in August of 2001.

Nick Terrill  
Daresbury Laboratory

### CCP13 and NCD Training Workshop, 23rd-24th November 1999, Daresbury Laboratory

A training workshop was held at Daresbury Laboratory on 23rd-24th November, 1999, to demonstrate data collection and analysis in fibre diffraction and non-crystalline diffraction experiments. This workshop was targeted primarily at new PhD students and post-doctoral researchers who were unfamiliar with fibre diffraction and

SAXS/WAXS data collection techniques and the tools available for data reduction and analysis in the CCP13 and non-crystalline diffraction (NCD) software suites.

The workshop commenced with an introductory lecture by Nick Terrill followed by a demonstration



Delegates at the first CCP13 and NCD Training Workshop at Daresbury Laboratory, 23<sup>rd</sup>-24<sup>th</sup> November 1999.

of SAXS/WAXS and fibre diffraction data collection on stations 8.2 (Nick Terrill and Anthony Gleeson) and 7.2 (Rob Kehoe) respectively. On the 24th November, there was a full day's training in the use of CCP13 and NCD software with demonstrators Mark Shotton, Richard Denny, Nick Terrill and Anthony Gleeson. This covered the reduction of one-dimensional NCD data using XOTOKO and its analysis using the XFIT and CORFUNC programs. Data format conversion and the preliminary analysis of two-dimensional fibre diffraction data using XCONV and XFIX were demonstrated along with the use of the 2-D pattern-fitting program, LSQINT. A total of 17 PhD students and post-doctoral

researchers attended the workshop, which was received very positively. It is now planned to stage the software training workshop as an annual event and some delegates also voiced their interest in an advanced software training course. Notification of further workshops will be published via the CCP13 bulletin board (to subscribe to the bulletin board, see <http://www.dl.ac.uk/SRS/CCP13/subscribe.html>). All CCP13 software can be downloaded from <http://www.dl.ac.uk/SRS/CCP13>

Mark Shotton  
Daresbury Laboratory

### Denver X-ray Conference, August 1999, Steamboat Springs

If you ever get an invite to the Denver X-ray Conference at Steamboat Springs, drop everything and take off for a week, it's a brilliant place for a conference. You would be advised to make your travel plans well in advance as this is about as American as public transport gets. I arrived fresh from a ten hour flight via Dallas (thanks to American for upgrading me to business class) to be greeted by howls of derision when I enquired about getting to Steamboat Springs via public transport. The conference title is a little misleading, it is an annual event, normally held in Denver but every three years or so it migrates to Steamboat Springs for a larger event and all the family members join in. I use migrates wisely as Steamboat Springs is 170 miles (280km) from Denver and after 5pm there is no public transport in summer unless you book in advance. Well you live and learn, so a hire car it was. The drive to Steamboat is fairly simple, onto the interstate, turn right at interstate 70, drive for a few hours, turn right onto 9, drive a few more hours and Bob's your uncle, you're at the hotel, no problem, except for the suicidal deer of course, but that goes without saying, oh and it was dark by this point, but hey who's counting.

Steamboat Springs spends most of the winter wrapped in a blanket of snow and is known for its skiing and winter sports. It is placed in a very picturesque setting on the side of the Rockies at about 9000ft (2750m). It's not far from Walton Creek; I was expecting John Boy to drive round the corner every time I went for a walk. The hotel (The Sheraton, reasonable rates over summer) sits at the

bottom of the major cable car route. The cable car is a pleasant 10 minute journey to the top of the mountain where the first day started with a Plenary session chaired by Randy Barton of DuPont and Vic Buhrke of The Buhrke Company. The conference is very broad in nature covering both diffraction and spectroscopy. Due to the large number of industrial members, powder diffraction has a large slice of the cake, with single crystal, SAXS and spectroscopy making up the remainder. However, the plenary sessions, being open to all, were of an exotic flavour covering uses of X-rays in space, from the growing of protein single crystals and their examination with the Bede system ([www.bede.com](http://www.bede.com); [www.nasa.gov](http://www.nasa.gov)) to X-ray detectors in space. Thus the start gathers many of the participants up to the top of the mountain for the opening. The plenary session lasts until lunch with the remainder of the day back in the hotel. To descend the mountain you can either take the serene cable car or, as many of the members decided, take up the \$10 challenge. Just outside the hall, a mountain bike rental was doing brisk business, hiring out bikes for one-way to the bottom, this is the kind of sport I can just about manage, let gravity do all the work for you and hope friction doesn't let you down. You get 1 hour for the journey down, it can be done in about 25 minutes if you are suicidal. The journey is along a sheep track with innumerable concealed hairpin bends, foot deep ruts and shear drops, but well worth it and I highly recommend it. On reaching base camp, there is time for a quick shower and a spot of lunch on the terrace outside Starbucks before the rest of the day's talks.

I was kindly invited by Randy and Ben Hsiao to talk in the *Polymers II: In Situ Scattering/Diffraction Characterization of Polymers* session about the work we have been doing at Daresbury on 16.1 with the extruder and to talk a little about the available software in the CCP13 suite. Due to the high number of powder diffraction users I thought it prudent if I also mentioned the CCP14 powder diffraction suite as well. The session I was involved with covered mainly extrusion and simultaneous studies of polymer crystallisation. We heard from Dr Mahendrasingam from Keele on their DL synchrotron studies as well as many U.S. and international contributors in the field. The full program can be found at <http://www.dxcicdd.com/99/default.htm> The discussion focused heavily on the use of synchrotron radiation to study polymer phase transitions before and during crystallisation

with work presented by Prof. J.M. Schultz, University of Delaware, Prof. B.S. Hsiao and myself to name a few.

Later that evening I looked up an old friend from my undergraduate days. He used to live in Birmingham, but moved to Denver about 4 years ago. He works for Bede and has always held a fascination for quantum mechanics; he is currently doing a great impression of the first spherical harmonic (physics joke) due to the rich food. We spent the evening of the conference dinner reminiscing about old times as the sun set over the mountains and we were bathed in the warm orange glow. It's hard work this. I will definitely be going back.

Patrick Fairclough  
University of Sheffield

### 8th Annual CCP13 Workshop, 15th –17th June 1999, St Andrews

This year saw a change in venue for the workshop which moved away from Daresbury to St Andrews in celebration of the Principal, Struther Arnott's 65th birthday and in honour of his contribution to fibre diffraction. John Squire who was retiring as chairman of CCP13, welcomed Trevor Forsyth as the new chairman and invited Prof. Arnott to begin the presentations with a plenary lecture entitled "Lessons for today and tomorrow from yesterday".

In this entertaining and informative talk, Prof. Arnott took us from a lesson in Scottish English to the more serious theme of the confidence in structures derived from fibre diffraction data. For example, collagen solved by crystallography shows no significant differences from the fibre work done fifteen years previously and oligonucleotide structures confirm the earlier results of fibre diffraction. The rest of the afternoon included talks on microfocus fibre diffraction experiments from Manfred Burghammer (ESRF) and a discussion of the opportunities for fibre diffraction on the new station 14.1 at the SRS, given by Liz Duke (Daresbury). The final talk of the day was given by Prof. Ian Ward (Leeds), who spoke about his work on elucidating the processes of fibre drawing and spinning, using data from both infra-red spectroscopy and X-ray diffraction. The day concluded with part one of the joint CCP13/NCD business meeting in which John Squire, in his role as editor of the CCP13 newsletter, *Fibre Diffraction*

*Review*, outlined the intention to scrutinize contributed articles more rigorously, using two referees per article. Greg Diakun updated the audience on developments in the NCD facility group and the requirements for microfocus experiments at Daresbury were discussed.

Richard Heenan (RAL) stepped into the breach to replace Gerald Stubbs (Vanderbilt) who had unfortunately been unable to leave the US due to the storms raging across the country. Richard described his procedures for modelling scattering from surfactant interfaces. Tim Wess (Stirling) described his work on uncovering the mechanism whereby elasticity in fibrillin occurs and was followed by Joseph Orgel (Stirling) who discussed the phasing of the meridional reflections from collagen. After coffee, Watson Fuller (Keele) described, in a complementary talk to Prof. Ward's, the small-angle scattering data collection techniques that the Keele group had developed to follow the processes of drawing and crystallisation in polymers. Anatoly Snigirev (ESRF) reported on developments in microfocus technology, particularly Fresnel optics and refractive optics, and their applications. Andy Hammersley (ESRF) discussed various user interface types employed in programs and their suitability in various applications. He then described the new "Files Series" interface in Fit2D, suitable for processing multiple data files.

Alan Windle (Cambridge) gave an account of work in his group on random co-polymers of PET and PEN. The slower crystallisation of these systems compared to the parent homopolymers made it easier to capture the characteristics of the crystallisation process. Adrian Rennie (King's College) described X-ray and neutron scattering experiments used to study phase transitions in the structure of dispersions of thin plate like colloidal particles. Mark Shotton (Daresbury and Imperial) giving his first account of his work as the CCP13 research assistant, described how the BSL/XOTOKO file format had been made more flexible, as well as other changes to the CCP13 suite. Andrew Miller (Stirling) rounded off the day's talks by highlighting the increased effectiveness of X-ray studies on biological fibres by the developments in synchrotron radiation. He went on to discuss aspects of the analysis of collagen diffraction patterns, in particular the background which appears to have a strong contribution from the unsampled molecular transform. On a very topical note, Andrew reminded the audience of work carried out in the 1960s which brought to light rearrangements of membrane lipids when cells keratinise and its bearing on recent work suggesting that X-ray diffraction patterns from keratin can be used to assess the propensity of patients to contract breast cancer.

Part two of the CCP13/NCD business meeting concerned the composition of the CCP13 Steering Committee. Tim Wess was re-elected and three others, Patrick Fairclough, Steve King and David Blundell were co-opted on to the committee. A series of short poster presentations followed: Sue Slawson (Daresbury) on the *DARTS* service, Colin Crook (Sheffield) on adhesives, Corinne Salou (Sheffield) on reflectivity of copolymer films, Hind Al-Khayat (Imperial) on insect flight muscle and Carlo Knupp (Imperial) on combined electron microscopy and X-ray diffraction of dog fish egg case.

Prior to the bus leaving for the conference dinner, there was time for the poster session and the software demonstration. The dinner, which was of a very high standard, took place in the imposing surroundings of Lower College Hall, with portraits of the present and former principals of St Andrews looking on. The present principal was also there in person and Prof. Arnott gave an entertaining impromptu after dinner speech having been thanked for his hospitality by Trevor Forsyth. Prof. Arnott then presented the cheques to the winners of the poster competition.

These were Carlo Knupp (Imperial) in the biology category and Erno Klop (Akzo Nobel) in the synthetic polymer category.

Thursday morning began with an account by Tim Lodge (Minnesota) on the effects of solvent on block copolymers and their structure in solution. A systematic study of styrene-isoprene diblock copolymers dissolved in a series of di-alkyl phthalates was undertaken, using SAXS to reveal the symmetry of the structures and SANS to determine the selectivity of the solvent and its distribution within the structure. These experiments show that the effect of neutral solvent in stabilizing disordered states, suppresses the order-disorder transition more than has been predicted by theory. Tony Ryan (Sheffield) described experiments to elucidate reaction-induced phase separation in PPE. Peter Timmins (ILL) discussed the application of contrast variation neutron scattering experiments to troponin, one of the proteins making up the thin filament in muscle. John Squire continued the muscle theme, describing various approaches to finding the binding states of myosin to actin using combinations of electron microscopy, time-resolved SAXS and structures from single crystal studies. Athene Donald (Cambridge) ended the talks with a discussion of the properties of starch. Both SAXS and SANS were used to provide complementary information: SAXS to follow real-time processes and SANS to show the distribution of solvent.

Trevor Forsyth made his concluding remarks as the new chairman of CCP13, first stressing that the CCP13/NCD workshop was not just about fibre diffraction but encompassed a wide range of experimental techniques. He wished Professor Arnott a happy birthday and thanked him and the staff of St Andrews for their hospitality. Trevor also thanked John Squire for getting CCP13 off to such a good start and for his willingness to continue his involvement on the CCP13 steering committee and as editor of the *Fibre Diffraction Review*, the CCP13 newsletter. Trevor reminded the audience that the newsletter is open to articles from all and that a more rigorous refereeing procedure was to be put in place. Finally, Trevor thanked Alison Mutch and Sue Waller for all their work in making the workshop run smoothly and Mark Shotton presented them with bouquets.

Richard Denny  
Daresbury Laboratory



**Photographs of the 9th annual workshop:** The CCP13 Steering Committee meeting, delegates enjoy a lively poster viewing session, poster prizes are awarded by Professor Struther Arnott after the conference dinner.

# Technical Developments

## Beamline 14 and the Opportunities for Fibre Diffraction

E.M.H. Duke

Daresbury Laboratory, Daresbury, Warrington WA4 4AD, U.K.

Beamline 14 is the new beamline currently in the final stages of commissioning on the Synchrotron Radiation Source (SRS) at Daresbury Laboratory. The beamline has two stations, principally for protein crystallography. However one, Station 14.1, will be able to accommodate the fibre diffraction work that is currently taking place on Station 7.2.

The multipole wiggler (MPW) used to provide radiation for beamline 14 has 9 poles, with a nominal field strength of 2.0T, and 2 side poles. The maximum length of straight section available in the second generation SRS governs the MPW length of 1m. The operating magnet gap of 20mm was determined by studying the effect of a restricted aperture on the lifetime of the electron beam in the SRS.

Calculations were done to establish suitable positions on the radiation fan for the two stations. The peak flux from the MPW is at the centre of the fan; between the centre of the fan and 6.5mrad the flux drops by an order of magnitude, highlighting the importance of positioning the stations as close to the centre of the fan as possible. If one station were to be positioned at the centre of the fan and the second offset then the second station would have

significantly less flux than the first. However by offsetting the central station slightly from the centre of the fan, allowing the second station to be more central, the gain in flux for the second station more than compensates for the slight loss of flux in first station. Therefore, Station 14.2, the more intense station takes beam from +3mrad to -1mrad and Station 14.1 from -1.5mrad to -4.5mrad. It is possible for the two stations to be separated by only 0.5mrad by having the beam for Station 14.2 crossing over the top of the beam for Station 14.1. This allows the dead space on the outside of the radiation fan to be used for all the cooling and bending mechanisms. The outline of Beamline 14 shown in Figure 1 illustrates this.

In order to ensure swift beamline construction a simple optical design for both stations was chosen. Thus Stations 14.1 and 14.2 both have vertical focusing provided by a 1.2m silicon cylindrical mirror coated in rhodium. The horizontal focusing and monochromation is provided by a single bounce, 300mm long, Si 111 monochromator. Both optical elements are water-cooled. In addition the effect of the single bounce monochromator, to deflect the beam out sideways, allows the two stations to be fitted into the limited space available for the

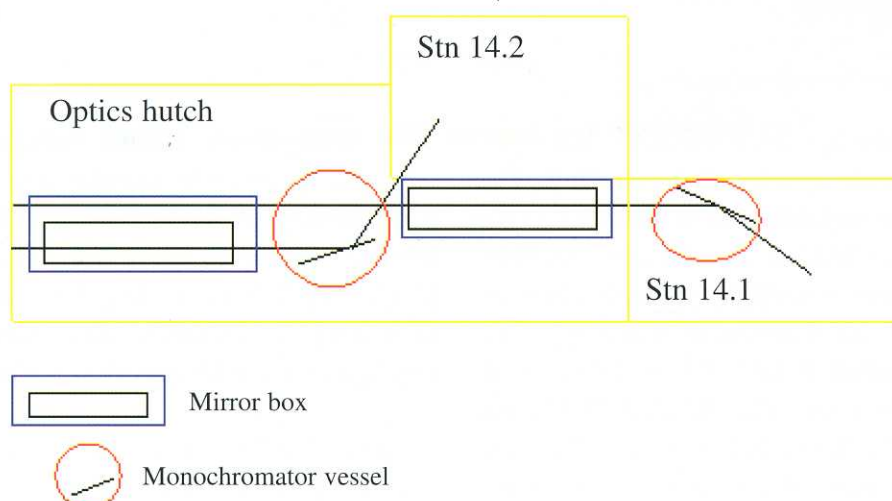


**Figure 1:** Schematic layout of BL14

beamline.

The optical configuration chosen tends to lead to operation at a single wavelength. However a system has been developed where two monochromator crystals optimized for 2 different wavelengths are mounted in the vessel in a double-decker arrangement. This allows the wavelength to be changed simply by translating between the two monochromators. The two wavelengths of operation for Station 14.1 are 1.2Å and 1.5Å. Table 1 gives an impression of the relative flux expected on Station 14.1 compared to the existing fibre diffraction station, Station 7.2.

Station	Relative Intensity
7.2/9.5	1
9.6	10
14.1	10-20
14.2	20-40
BM14 (ESRF)	20

**Table 1:** The Relative Intensity of Beamline 14 Stations

It is planned that initially the existing fibre diffraction equipment from Station 7.2 will be transferred to Station 14.1. The rotation camera on

Station 14.1 was designed and manufactured at the EMBL in Hamburg, an earlier model is currently in use on Station 7.2. Initial commissioning of the station will be done using a MAR 30cm image plate detector. Ultimately an ADSC Quantum 4 CCD detector will be mounted on the station. This is a 180mm x 180mm 2 x 2 array of CCDs with a full-frame slow readout time of 9s. This drops to 3s if the fast readout option is used.

Plans are underway to develop a new fibre camera specifically for Station 14.1. Currently users' opinions are being sought on various design features such as sample alignment, helium beam path both before and after the sample, and the ability to move the sample in different planes. An outline design of the camera will be available by the end of March. This will then be refined before being manufactured to be available at the end of July. Anyone wishing to provide input into the design of the camera should get in touch with Rob Kehoe at Daresbury Laboratory (tel. 01925 603626, email r.c.kehoe@dl.ac.uk). Relevant web pages can be found via the Protein Crystallography web pages at <http://www.dl.ac.uk/SRS/PX/index.html>. The new Station Manager for Station 14.1 is Mike MacDonald (tel. 01925 603627, email m.a.macdonald@dl.ac.uk). The Station Deputy is Rob Kehoe (tel. 01925 603626, email r.c.kehoe@dl.ac.uk).

### POLO Detector: 5 CCD SAXS/WAXS Area Detector for Synchrotron Radiation

J.P.A. Fairclough<sup>1</sup>, A.J. Ryan<sup>1</sup>, A.N. Allinson<sup>2</sup>, B. Pokric<sup>2</sup>, G. Long<sup>3</sup>, K Moon<sup>3</sup>, B.R. Dobson<sup>4</sup>, W. Helsby<sup>4</sup> and G.E. Derbyshire<sup>4</sup>

<sup>1</sup> Department of Chemistry, University of Sheffield, Sheffield, S3 7HF

<sup>2</sup> Electrical Engineering and Electronics, UMIST, Manchester M60 1QD

<sup>3</sup> York Electronics Centre, University of York, York

<sup>4</sup> CCLRC Technology Division

A novel area detector for SAXS/WAXS has been developed for use with synchrotron radiation. The detector is in fact two separate entities: one CCD for SAXS and 4 CCDs for WAXS. The detector has been designed to allow the simultaneous collection of time-resolved small and wide-angle scattering. The detector is based around 5 EEV 05-30 CCDs with resolution of 175µm each. The WAXS CCDs are angled at 22.5% to the X-ray beam, in a 2x2 mosaic with a hole at the centre of the array to allow the small angle signal to be transmitted to the SAXS detector at the rear of the instrument, see Figure 1.

This arrangement allows the WAXS detectors to completely cover an angular range of 5° to 45° with a resolution of 0.05°. Using the diagonals of the mosaic, data up to angles 61° can be collected. Both WAXS and SAXS detectors are simultaneously collected at 30MB/s data rate, allowing time resolution down to approx 6 frames per second.

Each pixel value is digitised using low and high gain. The high gain channel has an adjustable offset allowing improved signal to noise characteristics for the selected range. This is particularly useful for

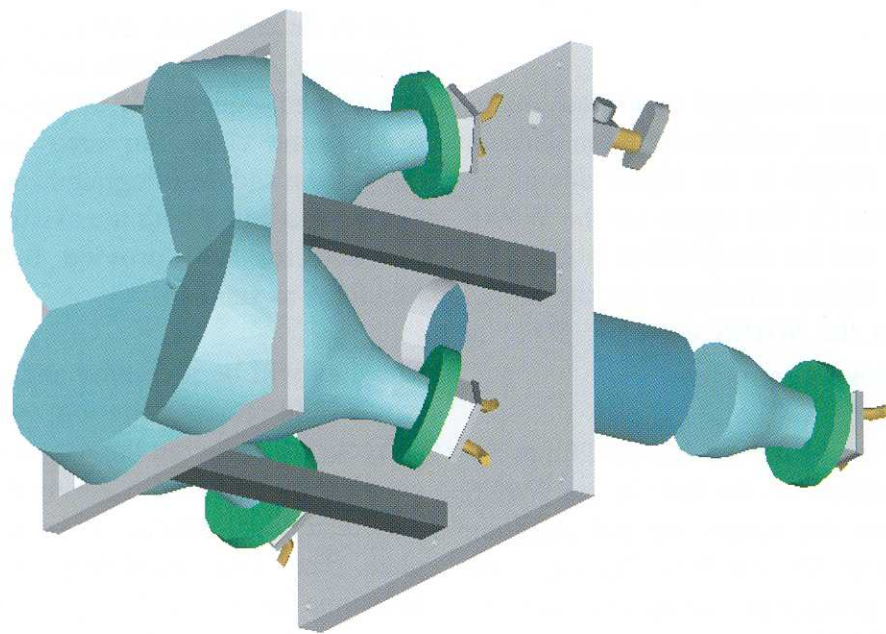


**Figure 1:** Schematic showing layout of the CCD tapers for WAXS and SAXS.

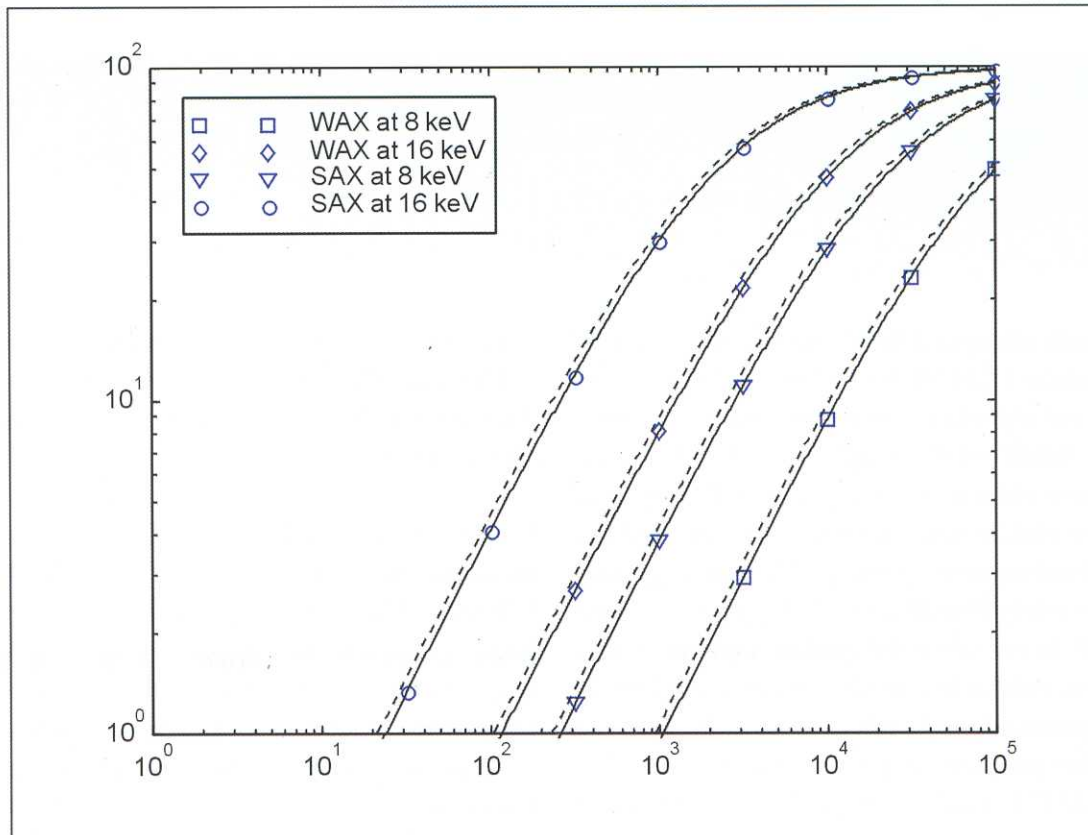


**Figure 2:** Detector Quantum Efficiency (DQE) as a function of intensity and photon energy.

discerning weak peaks in a high background as the high gain can be offset to the required background level.

The instrument has been developed to take advantage of station 16.1 at the SRS, with the optimum detector quantum efficiency (DQE) in the higher energy 16 keV range (see Figure 2). The tapers for the WAXS detectors are 3.88:1 and for the SAXS it is 2:1. This results in a slightly higher efficiency for the SAXS detector (90%) than the WAXS detector (80%) at 16keV and  $2 \times 10^4$  photons per pixel.

The SAXS detector can be moved from 0.27m to 3m from the sample position. As the hole in the WAXS mosaic is offset from the centre, the full quadrant from the beam stop to  $45^\circ$  can be collected at the 0.27m position. A transparent beam stop will be mounted before the SAXS detector for the collection of normalisation data. The detector is designed to fit seamlessly into the existing Daresbury instrumentation. This will allow the SAXS detector to be replaced by the RAPID SAXS detector, if required.

In normal operation, data will be written to a 20Gb RAID ultra wide SCSI array allowing 2000 frames of data to be collected, before downloading the NCD file server. At slow frame rates, the full image of the data can be sequentially displayed on the console. At high frame rates, an area can be selected for integration and the integrated count can be displayed. For compatibility with the existing Daresbury set-up, the detector will provide the cycle and group functions as standard.

The data will be presented and saved with dark and white-field corrections but without geometrical corrections, allowing the user to select the preferred geometrical corrections during data reduction. These may be a transformation to reciprocal space or a flat plate. The data correlating each pixel to angular position, to allow these transformations to be performed, will be stored separately from the data set as is currently the case on existing equipment.

This detector is scheduled for delivery for January 2000 and should be available as a scheduled instrument shortly afterwards.

## CCP13 Software Development

M.W. Shotton and R.C. Denny

Daresbury Laboratory, Daresbury, Warrington WA4 4AD, U.K.

*There has been an upgrade of the existing CCP13 program, corfunc (T.M.W. Nye 1994), which can be used to perform correlation function analysis of one-dimensional small-angle scattering (SAXS) data. corfunc is now driven by a Java-based graphical user interface (GUI) and incorporates more robust non-linear least-squares fitting. The GUI greatly enhances the user-friendliness of the program and also allows it to be run with greater efficiency and flexibility. New interactive graphics allow corfunc to be run independently of other programs such as XOTOKO. The program is provided to run on NT / Windows, LINUX and various UNIX operating systems.*

function is simply the Fourier Transform of the SAXS curve as shown in Figure 1.1. It is related to the electron density distribution within the sample as shown in Figure 1.2.

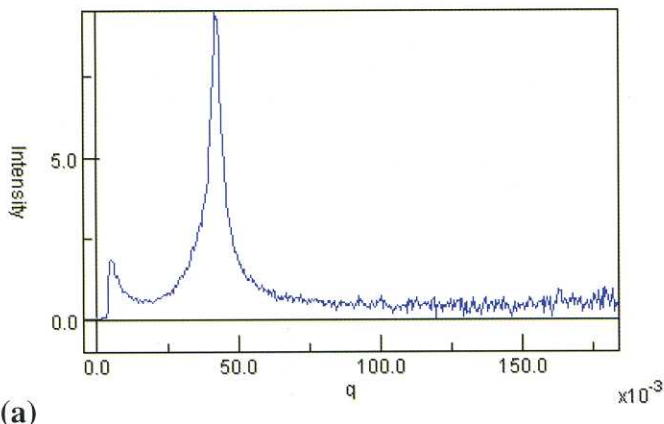
Figure 1.3 shows the structural parameters that can be obtained by interpretation of the 1-D correlation function. This interpretation assumes that the sample has an ideal lamellar morphology, *i.e.* it assumes that the sample consists of an ensemble of isotropically distributed stacks of alternating crystalline and amorphous lamellae. The stacks are assumed to be of dimensions that are large enough not to affect the small angle scattering.

## 1 Introduction

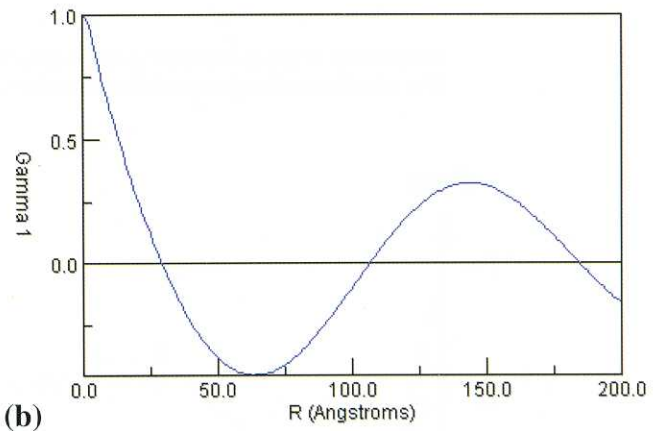
SAXS data can be subjected to correlation function analysis in order to derive structural parameters corresponding to the sample [1-2]. The correlation

## 2 The corfunc GUI

The Java-based GUI that drives the corfunc program (see Figure 2.1) can be run on any Java 1.2 platform or above (see <http://www.javasoft.com>). SAXS data



(a)



(b)

**Figure 1.1:** (a) One-dimensional SAXS data, (b) One-dimensional correlation function calculated as the Fourier Transform of the SAXS data using the *corfunc* program.

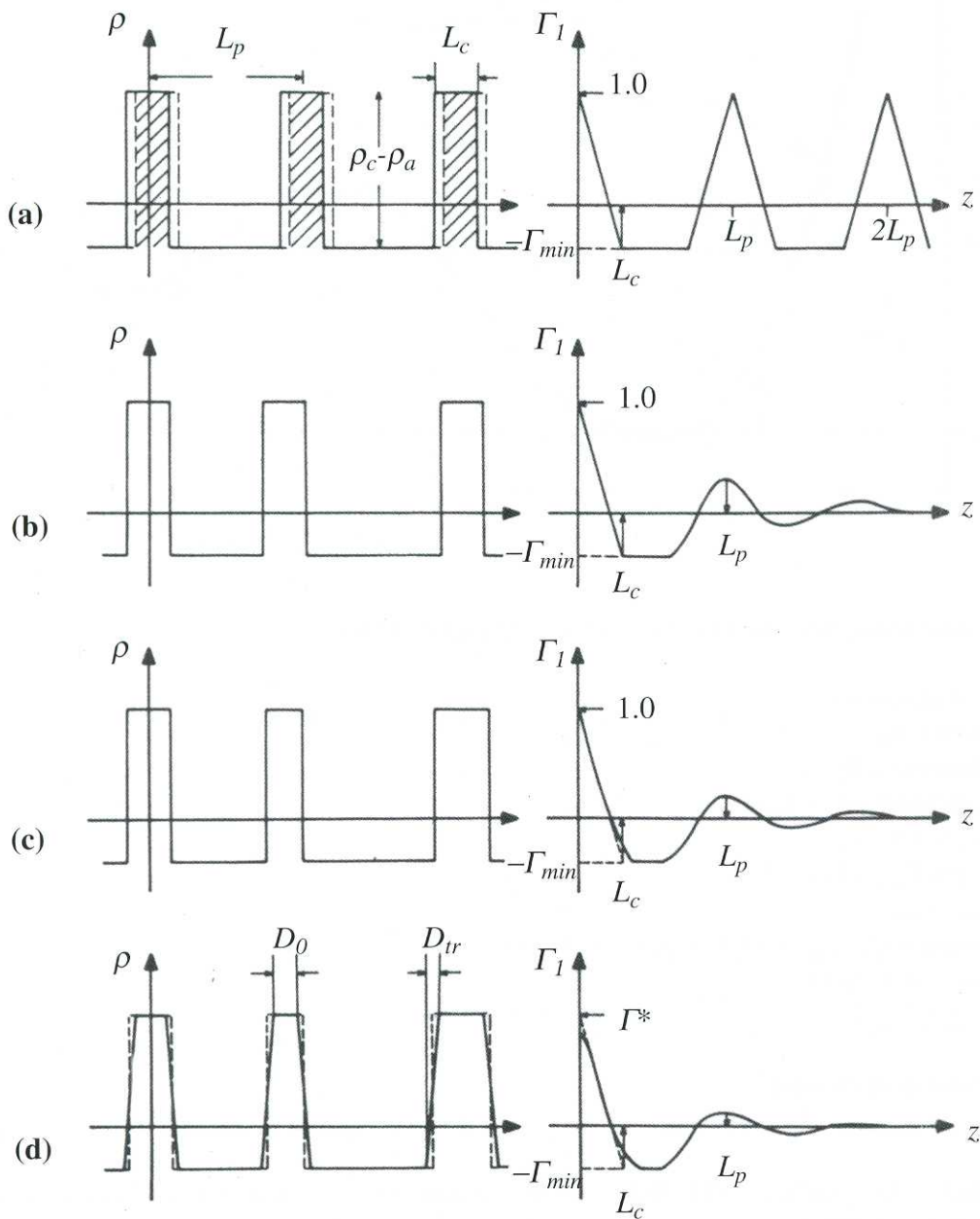


**Figure 1.2:** Electron density distribution  $\rho(z)$  and its related correlation function  $\Gamma_I(z)$  for lamellar systems of different regularity [1]. (a) Periodic two-phase system. (b) The effect of long-spacing variations on (a). (c) The effect of thickness fluctuations on (b). (d) The effect of introducing diffuse phase boundaries to (c). Symbols are described in the caption to Figure 1.3.

**Extraction of ideal lamellar parameters from  
the one dimensional correlation function.**

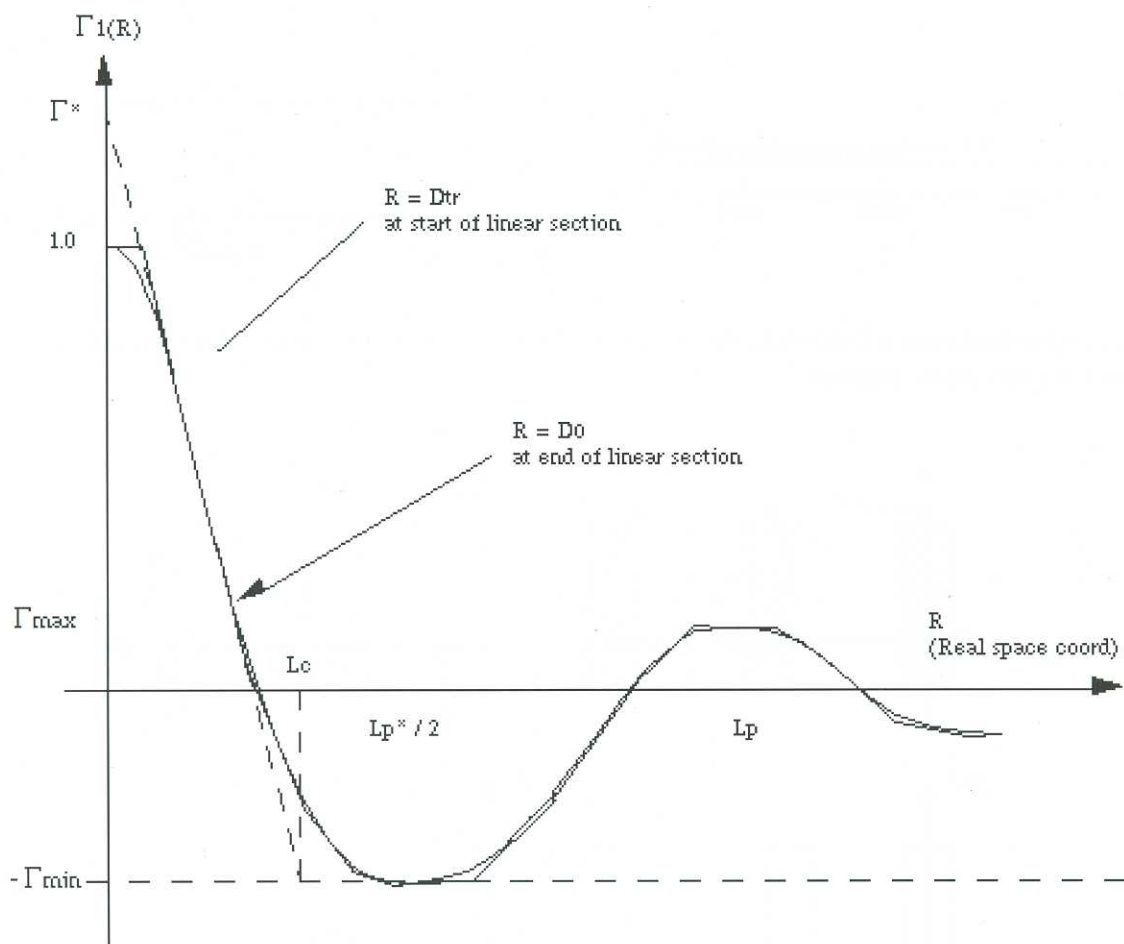


**Figure 1.3:** One-dimensional correlation function analysis. Parameters obtained:

Long period =  $L_p$

Average hard block thickness =  $L_c$

Average core thickness =  $D_0$

Average interface thickness =  $D_{tr}$

Average soft block thickness =  $L_a = L_p - L_c$

Local crystallinity =  $\varphi_l = L_c / L_p$

Bulk crystallinity =  $\varphi = \Gamma_{min} / (\Gamma_{min} + \Gamma^*)$

Polydispersity =  $\Gamma_{min} / \Gamma_{max}$

Electron density contrast =  $(\rho_c - \rho_a)^2 = (\Delta\rho)^2 = Q\Gamma^* / (\phi(1 - \phi))$

Specific inner surface =  $O_s = 2\phi / L_c$

Non-ideality =  $(L_p - L_p^*)^2 / L_p^2$

where  $Q$  = second moment or invariant

can be loaded in either OTOKO (see <http://www.srs.dl.ac.uk/NCD/computing/manual.otoko.html>) or ASCII format and are displayed as shown in Figure 1.1. By editing the various input parameters (see Figure 2.2) and then selecting items from the *Actions* menu, the user can perform

consecutively the three stages involved in the correlation function analysis:

- (i) extrapolation of the data to  $q = 0$  and  $q = \infty$
- (ii) calculation of the Fourier transform of the extrapolated data

(iii) interpretation of the correlation function obtained in (ii)

The results of the analysis are displayed graphically in pop-up windows or as scrolling text in the message window. Graphs can be saved in several common image formats. All results are also output to OTOKO and/or ASCII format files. Help pages are displayed in a platform-independent way using the JavaHelp system.

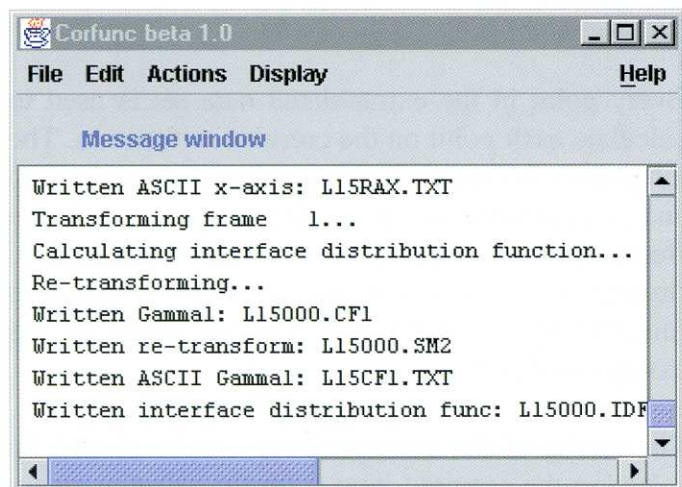


**Figure 2.1:** The *corfunc* GUI

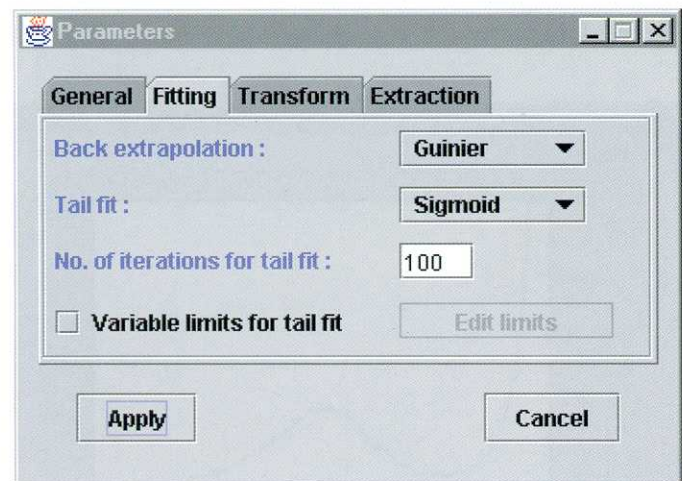


**Figure 2.2:** Input parameters

### 3 Data processing

#### 3.1 Extrapolation of SAXS data

Prior to calculating the Fourier Transform of the SAXS data, the data must first be extrapolated to  $q = 0$  and  $q = \infty$  to avoid the introduction of series termination errors in the transform.

##### 3.1.1 Extrapolation to $q = \infty$

Extrapolation to  $q = \infty$  is performed by fitting either a Porod [3] or sigmoid [4] function to the tail of the SAXS data. In *corfunc*, the “tail” of the data is taken as those data lying between the two red limit markers on the right of the SAXS data graph as shown in Figure 3.1. These can be positioned interactively by dragging them with the right-hand mouse button. If these limits vary from frame to frame, in the case of real-time data, variable tail limits can also be chosen

Tail-fitting functions:

$$I(q) = B + \frac{K}{q^4} e^{-q^2\sigma^2} \quad \text{Sigmoid}$$

$$I(q) = B + \frac{K}{q^4} \quad \text{Porod}$$

where  $B$  = Bonart thermal background

$K$  = Porod constant

$\sigma$  describes the electron density profile at the interface between crystalline and amorphous regions.

The tail-fit affects the correlation function in the most important region for the extraction of ideal lamellar morphology parameters. Hence it is vital to obtain a good fit to this tail.

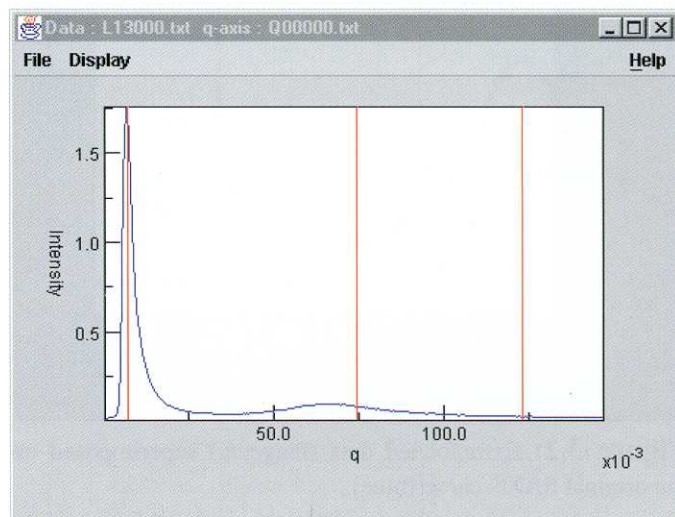


**Figure 3.1:** Selecting the fitting regions

##### 3.1.2 Extrapolation to $q = 0$

The data are extrapolated to  $q = 0$  by fitting a Guinier or Vonk model to the first few genuine data points after the beamstop. If the experimental data do not increase in intensity as the beamstop is approached, back extrapolation may fail. The first genuine data

point is indicated by the red limit marker on the left of the SAXS data graph as shown in Figure 3.1. This limit marker can be moved by dragging it with the right-hand mouse button. The *corfunc* program will attempt to set a sensible initial value for this limit.

Fitting functions for back-extrapolation:

$$I(q) = Ae^{Bq^2} \quad \text{Guinier}$$

$$I(q) = H_1 - H_2 q^2 \quad \text{Vonk}$$

### 3.1.3 Smoothing

The extrapolated data set consists of the Guinier or Vonk back extrapolation up to the first genuine data point, the original SAXS data up to the first tail-fitting limit and the sigmoid or Porod tail beyond this. It is shown as the magenta-coloured line in Figure 3.2. The join between the original SAXS data and tail-fit is smoothed using a Savitzky-Golay [5] smoothing algorithm that smooths the data without greatly altering higher moments. This avoids the formation of ripples in the correlation function that would occur with a period matching the d-spacing of the join. No smoothing is used at the join of the back-extrapolation to the SAXS data.

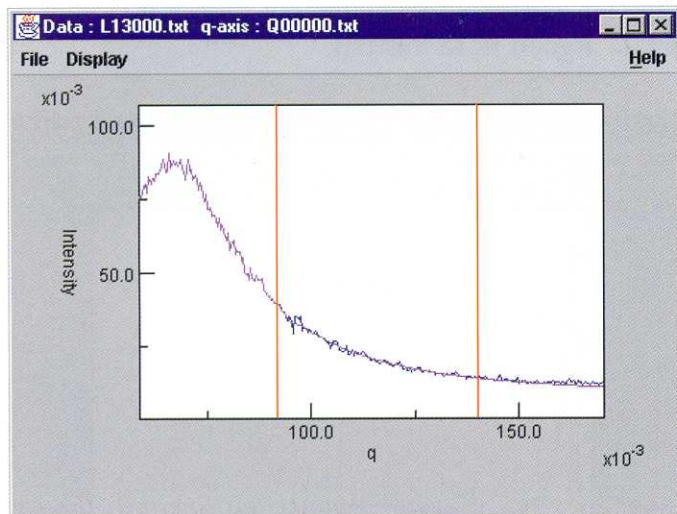


**Figure 3.2:** Extrapolated data (magenta) superimposed on the original SAXS curve (blue).

## 4 Calculating the correlation function

By selecting the *Transform* option from the *Actions* menu, the user may calculate the one-dimensional correlation function,  $\Gamma_1$  [2] (see Figure 1.1), the second moment of the data [2], the interface distribution function [7], and may re-transform  $\Gamma_1$  back into a scattering curve for comparison with the original data.

$\Gamma_1$  is given by:

$$\Gamma_1(x) = \frac{\int_0^\infty j(q)q^2 \cos(qx) dq}{Q}$$

where  $j(q)$  is the scattering intensity and  $Q$  is the second moment or invariant of  $j(q)$  given by:

$$Q = \int_0^\infty j(q)q^2 dq$$

Every point in the extrapolated data set is used to calculate each point on the correlation function. The integration is numerical (a trapezium approximation) and is performed up to  $q = 0.6$ . Together with the fluctuations introduced by this truncation, fluctuations are also introduced into the correlation function by the finite gap between points in the extrapolated data set.

The results of the transformation can be plotted by selecting the required item from the *Display* menu. In the case of the re-transformed correlation function, it will be added to the background found during the extrapolation process and superimposed on the original SAXS data for comparison (see Figure 4.1).

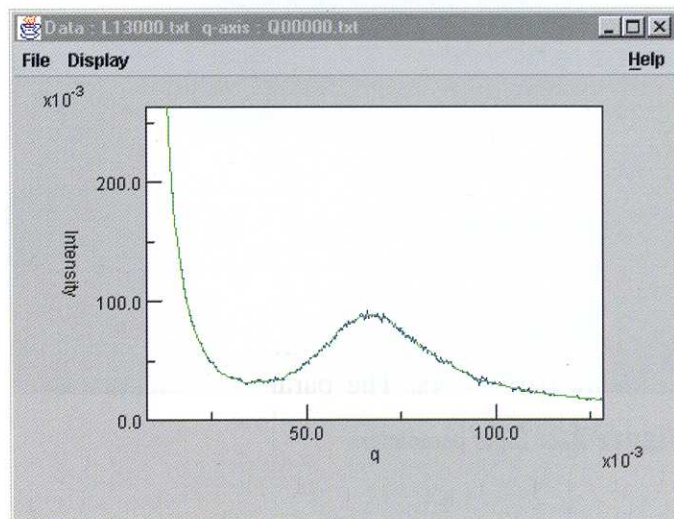


**Figure 4.1:** The re-transformed 1-D correlation function (green) superimposed on the original SAXS data (blue).

## 5 Interpretation of the correlation function

The user may interpret the correlation function by selecting the *Extract parameters* item from the

*Actions* menu. The correlation function is interpreted in terms of an ideal lamellar morphology [7] and structural parameters are obtained as shown in Figure 1.3. It should be noted that a small beamsize is assumed; no de-smearing is performed.

It is important to note that, according to Babinet's principle, in a two-phase structure such as the ideal lamellar morphology, the electron densities of the two phases (crystalline and amorphous) may be interchanged without affecting the scattering curve or correlation function [6]. Therefore, from correlation function analysis alone, we cannot distinguish between:

- $L_c$  and  $L_a$
- $\phi$  and  $(1 - \phi)$
- $\rho_c$  and  $\rho_a$

and these parameters may be interchanged, also affecting the other parameters derived from them.

It is also important to check that a horizontal section exists in the first minimum of the 1-D correlation function ( $-\Gamma_{min}$ ) as shown in Figure 5.1. This horizontal region is usually present when the sample crystallinity is < 30 % or > 70 %. In the intermediate region between 30 % and 70 % crystallinity, there may be no horizontal section, and in this case, the equation for the bulk crystallinity

$$\text{Bulk crystallinity} = \phi = \frac{\Gamma_{min}}{\Gamma_{min} + \Gamma^*}$$

no longer applies. In order to obtain reliable results for this intermediate crystallinity, other data are needed to complement the correlation function analysis [6].

If a Porod profile was used for tail-fitting, Porod analysis is performed after extraction of the lamellar structure parameters. The parameters calculated by the Porod analysis are given below:

Porod constant  $K$

Surface to volume ratio =  $\pi K \phi (1 - \phi) / Q$

Characteristic chord length  $l_p = 4Q / \pi K$

Crystalline chord length =  $l_p / (1 - \phi)$

Amorphous chord length =  $l_p / \phi$

where  $Q$  = second moment or invariant.

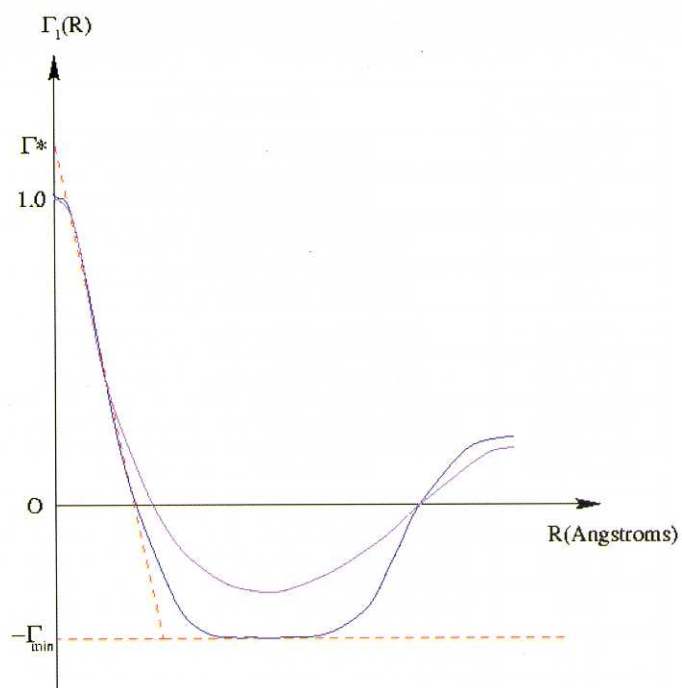


**Figure 5.1:** The 1-D correlation function shown in blue has a horizontal section in the first minimum, yielding the bulk crystallinity from the base line  $-\Gamma_{min}$ . The first minimum of the 1-D correlation function shown in magenta has no horizontal section and the equation for bulk crystallinity given above no longer applies.

## References

- [1] Strobl, G. R. and Schneider, M. J., *Polym. Sci.* (1980) **18**, 1343-1359.
- [2] Balta Calleja, F. J. and Vonk, C. G., *X-ray Scattering of Synthetic Polymers*, Elsevier Amsterdam 1989, 247-257.
- [3] Balta Calleja, F. J. and Vonk, C. G., *X-ray Scattering of Synthetic Polymers*, Elsevier Amsterdam 1989, 257-261.
- [4] Koberstein, J. and Stein R. J., *Polym. Sci. Phys. Ed.* (1983) **21**, 2181-2200.
- [5] Press, W. H. et al., *Numerical Recipes: the Art of Scientific Computing*, Cambridge University Press 1986.
- [6] Balta Calleja, F. J. and Vonk, C. G., *X-ray Scattering of Synthetic Polymers*, Elsevier Amsterdam 1989, 261-288.
- [7] Glatter, O. and Kratky, O., *Small Angle X-ray Scattering*, Academic Press Inc. London Ltd. 1982, 433-466.

## Summary of Available CCP13/NCD Software

<b>Program</b>	<b>Description</b>
XOTOKO	1-D data manipulation
BSL	2-D data manipulation
v2A	vax to unix data conversion
A2V	unix to vax data conversion
OTCON	ascii to otoko data conversion
RECONV	otoko to ascii data conversion
TIFF2BSL	image plate (tiff) to bsl conversion
BSL2TIFF	bsl to tiff conversion
i2A	ieee to ansi data conversion (DEC only)
XCONV	file format conversion (GUI-driven)
XFIT	1-D fitting and plotting (GUI-driven)
XFIX	fibre pattern analysis (GUI-driven)
CONV	file format conversion (command line)
FTOREC	reciprocal space transformation
LSQINT	2-D integration and background fitting
CORFUNC	correlation function analysis
SAMPLE	Fourier-Bessel smoothing
FDSCALE	scaling and merging of intensities
FD2BSL	intensity to bsl conversion

The tables list the currently distributed CCP13/NCD programs, available as executable modules. The dates refer to the last creation of the executable.

A LOQ2BSL conversion program, for ISIS neutron data to BSL format, is also available for Solaris platforms.

<b>Program</b>	<b>Solaris 2.7</b>	<b>Irix 6.2</b>	<b>OSF 3.2</b>	<b>Linux</b>
XOTOKO	28/11/97	30/05/96	29/04/97	-
BSL	02/05/97	21/03/97	27/04/97	-
v2A	19/05/95	-	-	-
A2V	19/05/95	-	-	-
OTCON	06/06/95	08/07/94	-	08/05/97
RECONV	06/06/95	31/10/94	-	08/05/97
TIFF2BSL	17/03/97	-	-	-
BSL2TIFF	21/03/97	-	-	-
i2A	n/a	n/a	29/04/97	02/05/97
XCONV	04/06/99	04/06/99	-	04/06/99 *
XFIT	10/07/98	10/07/98	10/07/98	10/07/98 *
XFIX	09/04/99	09/04/99	09/04/99	09/04/99 *
CONV	09/04/99	09/04/99	09/04/99	09/04/99
FTOREC	12/04/99	12/04/99	12/04/99	12/04/99
LSQINT	12/04/99	12/04/99	12/04/99	12/04/99
CORFUNC	26/10/95	26/10/95	-	26/10/95
SAMPLE	05/11/96	04/11/96	04/11/96	04/11/96
FDSCALE	05/11/96	04/11/96	04/11/96	04/11/96
FD2BSL	05/11/96	04/11/96	04/11/96	04/11/96

\* These programs have been tested on Slackware 3.4, SuSE 5.3 and RedHat 5.0 distributions of Linux.

## Lessons for Today and Tomorrow from Yesterday

S. Arnott

The University, St Andrews, KY16 9AJ, Scotland

*Many early X-ray fibre diffraction analyses were flawed by poor modelling rather than low quality data. This revelation should prompt the adoption of more standard methods of analysis to facilitate critical appraisals of both models and experimental observation in this field.*

### The needless tension between X-ray analysis of molecular structures in fibres and in crystals

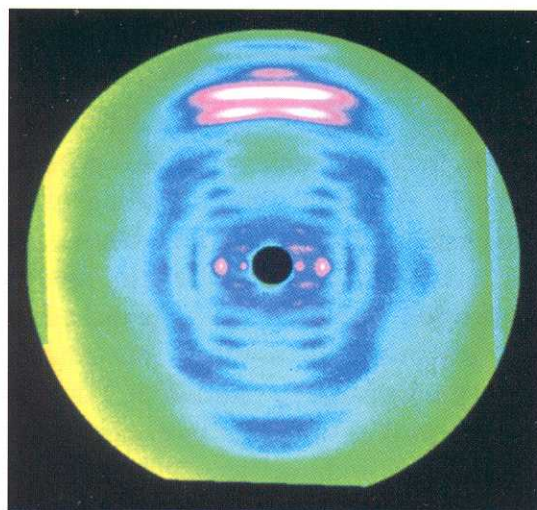
The molecular architecture of important linear polymers such as the polypeptide, polysaccharide and polynucleotide examples touched on below can be unveiled by X-ray diffraction analysis of their uniaxially oriented fibres that are sometimes further ordered in a variety of ways up to the level of microcrystals. Like almost all physical methods the technique has its idiosyncratic challenges, but its final requirement is production of a credible, parametrically parsimonious model that fits the observed data *significantly* better than any other plausible but parametrically equally parsimonious model. The accuracy of the final model should not be in doubt, but the precision of its description need be no greater than the use to which its parameters will be put. When appropriate and possible it is better to use X-ray diffraction analysis of single crystals with extensive three-dimensional order: with these the route to a unique (*i.e.* accurate) model is more facile and better understood among a wider group of practitioners; crystals also usually provide higher resolution data in larger numbers that lead to more precise and detailed structures.

For fibre diffractionists to concede the possible superiority of crystallographic analyses in certain circumstances is not to concede this in all circumstances, nor to provide a licence for later, merely authenticating crystallographic studies to airbrush from history the earlier pioneering discoveries of fibre diffractionists. To use

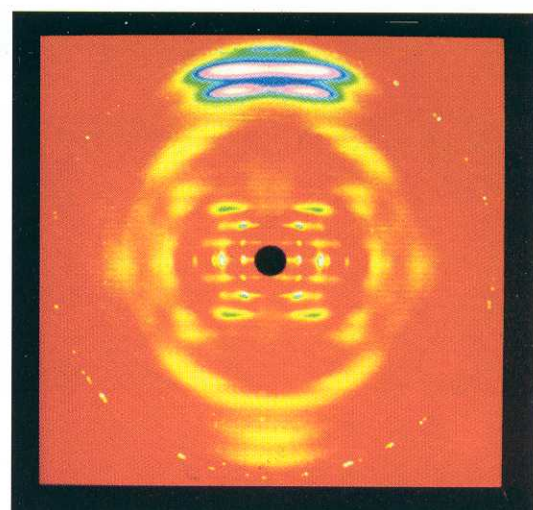
crystallographic analyses in such a fashion is not only intellectually fraudulent but also economically pernicious in diverting public funding from truly novel investigations. It is true, for example, that two decades of X-ray crystallographic analyses of oligonucleotide duplexes were launched by the dramatic discovery of a novel left-handed helix morphology accessible to oligo d(GC) duplexes [1] and, in a reversal of the usual sequence of events, a subsequent fibre study authenticated this discovery for similar polynucleotides [2]. But it is also the case that subsequent studies of oligonucleotide duplexes with more general sequences have shown that most are reluctant to crystallize and the few variants that do crystallize have overall secondary structures that differ insignificantly from the various B and A-type structures defined in fibres in earlier decades. The conformational excursions between one nucleotide and the next in these oligonucleotides are of the same order as was earlier observed between nucleotides in different fibrous allomorphs with a variety of helical symmetries [3]. Apart from the discovery of Z-DNA, crystallographic triumphalism in this area is especially inappropriate. Not only were the main B and A secondary structures defined and refined by fibre analyses decades before their re-description in oligonucleotides, but novelties like the heteromeric poly dR. poly rY structures [4] for DNA-RNA hybrids (Figure 1), and the achiral L-DNA duplex (Figure 2) have still to be sighted in single crystals. In such circumstances a sympathetic synthesis of the results of the two techniques should have been the more productive aim and outcome, but this has yet to occur.

### Collagen — another arena for collaboration?

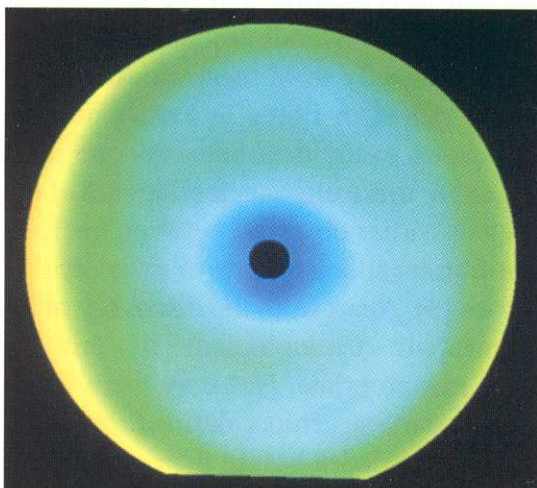
The canonical  $10_7$  triplex helix of collagen was defined authoritatively [5] in 1961 and refined using fibre diffraction data [6]. The first single crystal structure of a relevant oligopeptide, (hydroxypro-gly) $_{10}$ , was not determined until 33 years later [8] but its  $7_5$  triple helices merely authenticated Okuyama's (1981) quasi-fibrous structure [7] of (pro-hydroxypro-gly) $_{10}$  (Figure 3(a)) which was the first to reveal the alternative  $7_5$  triplex symmetry and show that collagen helices could be significantly dimorphic. These  $7_5$  triplets intriguingly have the same unit translation vertically as the  $10_7$  triplets (Figure 3(b)), but dramatically different rotations per



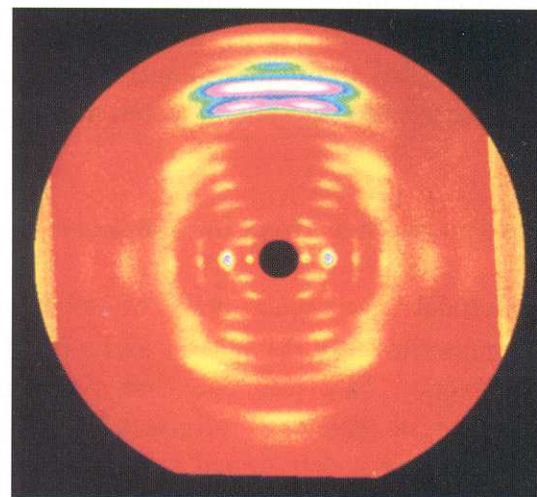
(a)



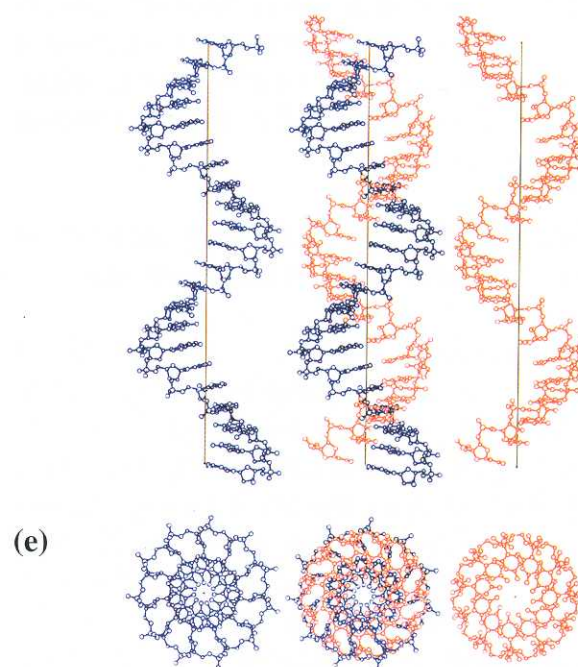
(d)



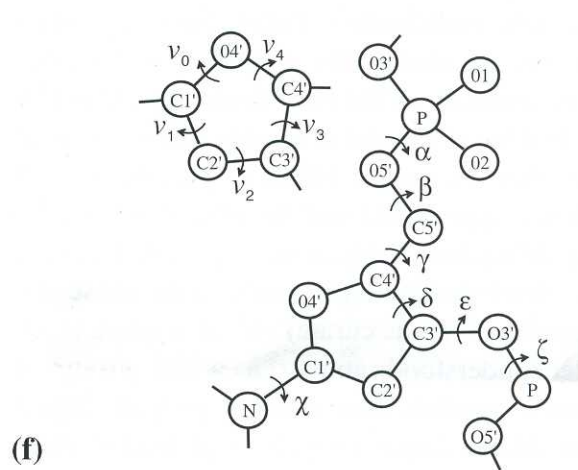
(b)



(c)

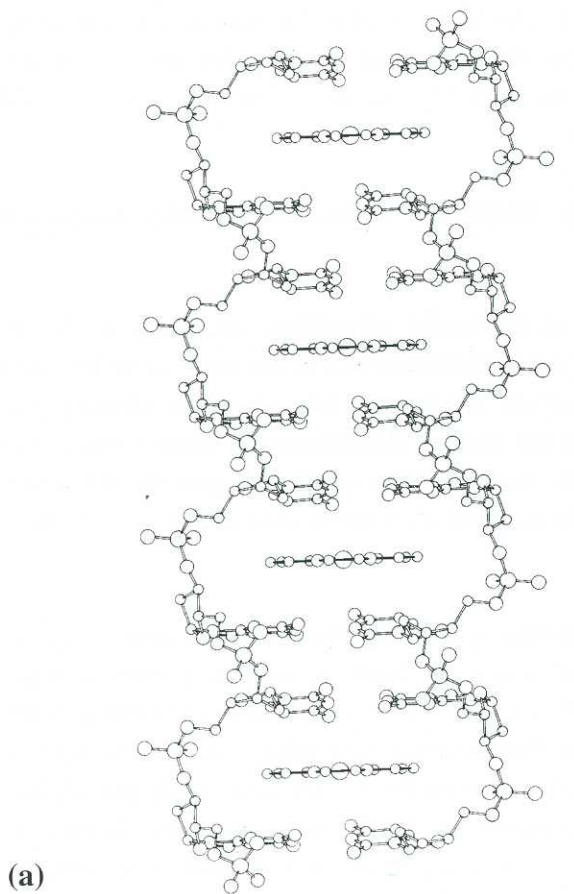


(e)

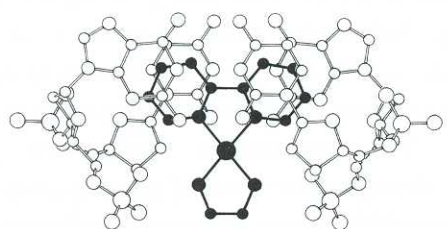


(f)

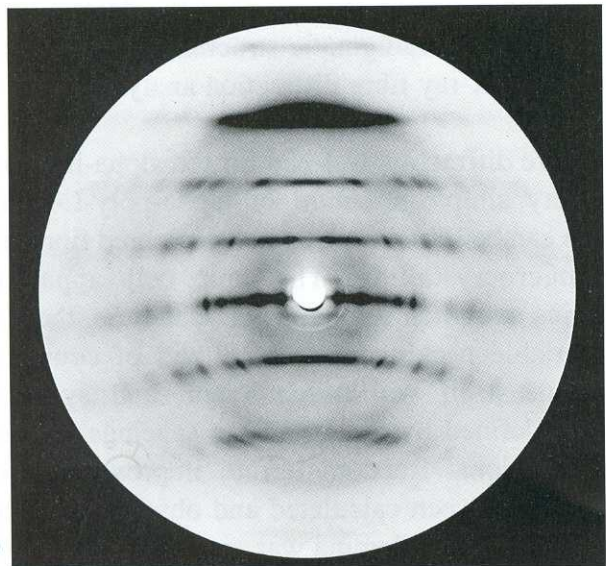
**Figure 1:** Modern methods of data collection using scanners and further processing by computers are illustrated by the sequence showing (a) a badly recorded X-ray fibre pattern from the synthetic DNA-RNA hybrid poly dI.poly rC, (b) the asymmetric background determined by sampling the interdiffraction space on the film record, and (c) the cleaned-up version of the pattern which shows the mixture of Bragg and non-Bragg diffraction from a screw-disordered uniaxially oriented array of 10-fold helices. A similar pattern from the 11-fold helices of poly dA.poly rU is shown in (d). Both patterns when analysed reveal duplex structures with non-identical iso-helical chains such as those for poly dA.poly rU shown (e) in two mutually perpendicular projections as a duplex and its deconstruction into two anti-parallel components. Such polymorphism even within a rather regular duplex should be a not unexpected feature of polynucleotides where even one residue (f) has many degrees of conformational freedom.



(a)



(b)



(c)

**Figure 2:** An exotic allomorph of the DNA duplex has a ladder structure (a) with no net twist over the periodicity of  $3 \times 3.4\text{\AA} = 10.2\text{\AA}$  which is the layer line spacing in the diffraction pattern (c). The bipyridyl-ethylene-diaminyl platinum intercalant that induces and supports this DNA structure is shown as filled circles in (b) which depicts the projection of the intercalated DNA complex down the long molecular axis.

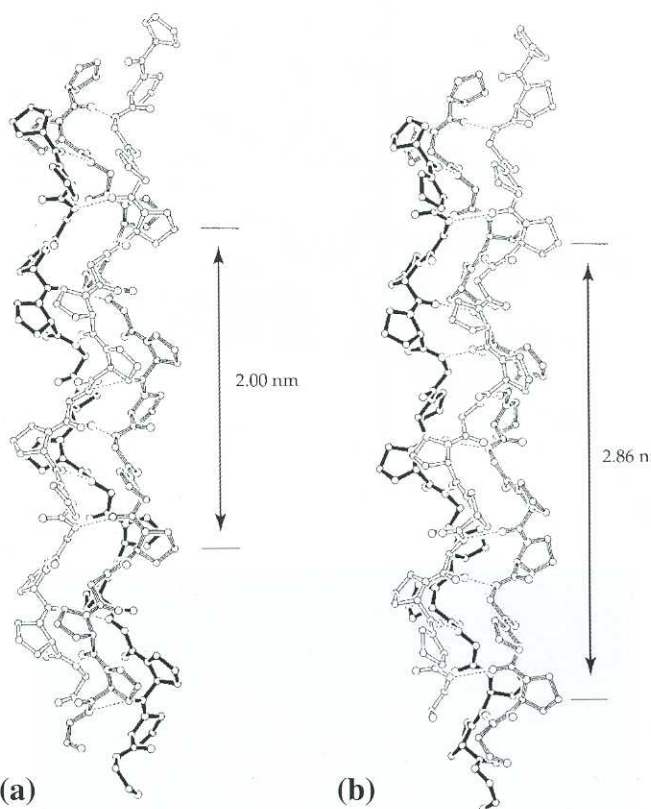
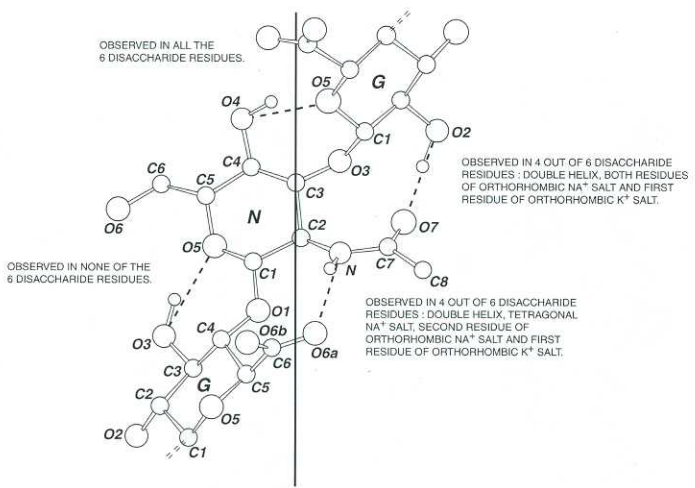


**Figure 3:** Two allomorphs of the collagen triple helix observed: (a) in a quasi-fibrous crystal of  $(\text{pro-pro-gly})_{10}$  [7] and in single crystals of  $(\text{hyp-pro-gly})_{10}$  [8] in which one gly in the middle of the sequence has been replaced by ala; and (b) in a native collagen. In the first allomorph the three polypeptide chains with  $7_1$  symmetry (twist  $51.4^\circ$ ) are nested to produce a triplex with  $7_1$  symmetry and unit height  $2.86\text{\AA}$  which is the same as in the canonical  $10_7$  triplex model in which the individual chains have  $10_1$  symmetry and a rather different twist ( $36.0^\circ$ ).

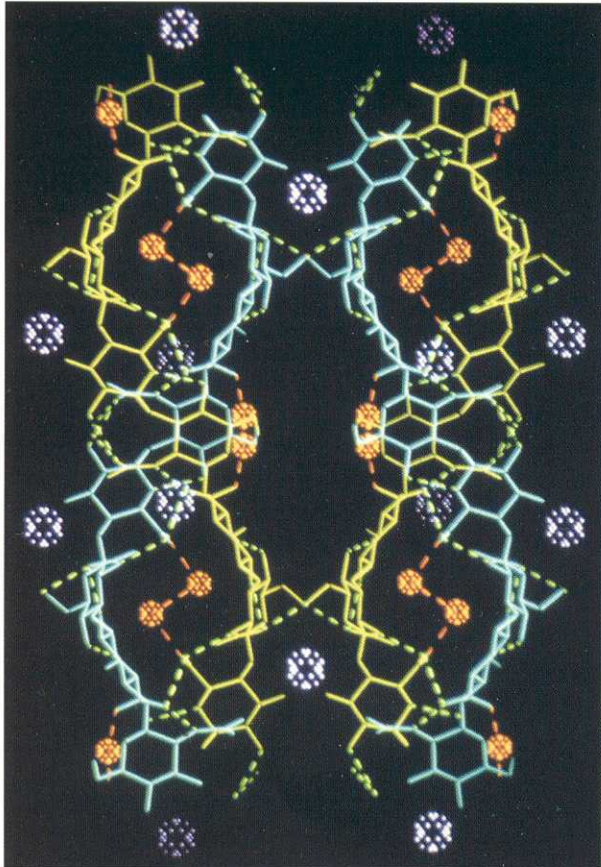
tripeptide ( $51.4^\circ$  and  $36.0^\circ$  respectively) in their individual  $7_1$  and  $10_1$  helical chains. This could be the mechanism whereby arrays of collagen helices of fixed length might optimize lateral inter-triplex contacts by different local rotations. More structures of differently sequenced, collagen-like structures in either fibres or crystals or both are needed to explore this peculiar polymorphism.

#### Polysaccharide structures are almost completely dependent on fibre studies

It is not surprising that extensive crystals are not found for such floppy, multifunctional, often polymorphic molecules [9], even when they contain multiple sources of chain stiffening as illustrated for hyaluronate in Figure 4(a). As a result of further stiffening by duplex formation (Figure 4(b)), which involves hemi-protonation, hyaluronate solutions can form a “putty” at pH  $\sim 3$  [10] when, theoretically,



(a)



(b)

**Figure 4:** It is possible (a) for the polydisaccharide units of hyaluronate and related connective tissue polysaccharides to be stiffened by multiple intramolecular hydrogen bonds [9] and (b) for hyaluronate uniquely to be further buttressed by double helix formation when hemi-protonated and interchain carboxyl-carboxylate and other hydrogen bonds are formed with the aid of special pairs of water molecules as revealed by fibre diffraction analysis [12]. These provide extra scaffolding for the duplex.

all the chains could be paired. *In vitro* at higher pH hyaluronate solutions exhibit anomalous viscosities, presumably because there is a persistent population

of stiff double helices. It is the anomalous viscosity that is the property that is exploited *in vivo* in the vitreous humour of the eye and in the synovial fluid of joints.

### Wrongly misprised data and rightly traduced models

Since it is the facile credibility accorded to X-ray single crystal structures that is the main contrast with fibre analyses it may be important to identify the source of the lack of confidence in fibre studies and if possible show that the credibility gap should never have been as wide as it seemed or is now less than it was.

Any community of experimental scientists that is small and wayward finds it hard to establish high credibility for its results, but those concerned with important biopolymer secondary structures had a particularly inauspicious start both with the alpha-helix of proteins and with commonest (B) allomorph of DNA. In both cases the initial molecular models were deemed to be essentially accurate from the beginning, but both failed to provide a good fit between the calculated amplitudes of diffraction and the corresponding amplitudes measured from fibre diagrams. The convenient conclusion that the relatively strange data were of poor quality and low information content was not easy to refute at the time and so the moments passed when the determination of two major paradigmatic structures could be fully credited to X-ray fibre diffraction analysis.

The fibre diffraction test-bed for the alpha-helix was the very simple structure of alpha-poly-L-alanine which can be spun into uniaxially oriented fibres that are microcrystalline. The unit cell apparently contains one pitch of one helical chain *i.e.* there are no variable packing parameters and of course the molecule itself with pitch length and symmetry readily defined by the layer line spacings has little conformational freedom left to improve the poor initial fit between calculated and observed structure amplitudes. The dilemma was resolved only in 1966 when it was shown [11] that the packing of alpha-poly-L-alanine consists of an array of its polar helices pointing up and down *at random*. The mutual displacement and orientation of the two sets of helices provide the two extra parameters needed to define the overall structure and the best values for these dramatically and significantly improve the fit between the model and observations.

The disjunction between model and data in the case of B-DNA was even more severe ( $R>0.8$ ) than for the alpha-helix but had a different source in the molecular structure itself and not the packing. The original Crick and Watson model [13] was entirely accurate in its principal features — the isomorphous AT and GC base-pairs, the right-handed  $10_1$  helix symmetry, the mutually intertwined, anti-parallel polynucleotide chains — but in one respect there was an error — the sugar rings were puckered in the C3'-*endo* fashion appropriate for A-DNA-like allomorphs rather than in the C2'-*endo* fashion characteristic of B-DNA-like structures. This error, of little interest at the time, has crucial consequences for the gross morphology of DNA models incorporating it: in particular, base-pairs have to be sited 4-5 Å further away from the helix axis than is indeed the case in B-DNA; this in turn produces a diffraction pattern very different in its intensity distribution from the one actually observed.

Yet again the quality of the unfamiliar diffraction data was made the scapegoat for the difficulty. But it could have been shown that the information content of the misprised data is in fact very high. Even when the observed amplitudes are combined disadvantageously in a strongly biased fashion with X-ray phases calculated from the morphologically flawed, aboriginal DNA model [14] the resulting Fourier synthesis clearly reveals the deficiencies of the model and makes clear that the remedy is a major relocation of the base-pairs (Figures 5(a), (b) and (c)).

Again the revisions took place rather too late for the damage to the credibility of X-ray fibre studies to be easily remedied. In the meantime, encouraged by the Watson and Crick modelling coup, which owed little to local experimental effort, many other analyses of fibrous polynucleotide systems were undertaken with just as little investment in experiment but with much less insight. Deservedly, most of the conclusions from these forays were wrong, but from them grew the myth that accurate X-ray fibre studies were impossible because of the appalling negative record that not one of these fibrous nucleic acid structures produced in the 1950s and 1960s by a laboratory not of Maurice Wilkins' school, has survived critical re-examination [16].

Despite this, the good news not only for fibre diffractionists, but also for all who need to rely on fibre-derived molecular structures, is that modelling

such structures with scrupulous application of today's technologies allows most gross errors to be detectable if enough effort is invested in alternative models. Very detailed structures and their subtle structural features can now be teased out routinely from data once unfamiliar to narrowly educated diffractionists.

## Conclusion

What should be clear is that the information content of X-ray diffraction data from fibres can be much higher than generally is conceded. What is needed is extra credibility for the conclusions derived from these data that has to come, in part, from analyses conducted within as standard a framework as possible so that results can be authenticated by a larger community of knowledgeable and sympathetic peers. The components of a modern fibre diffraction analysis include better specimen preparation, more intense X-ray sources, better data collection and handling, copious and fast computer facilities that trivialise the burden of refining and comparing all plausible alternative models (when the X-ray phase problem is not capable of experimental solution), standard frameworks for analysis such as linked-atom least-squares followed by statistical tests to adjudicate among competing models, a better awareness of the existence of structures with statistical or screw-disordered or other less than crystalline packings, and an ability to handle quantitatively the mixture of Bragg and non-Bragg diffraction that arises from such systems (e.g. Figure 1). A major effort to make and maintain all these procedures and processes within as uniform and standard a framework as possible would be of major benefit to the whole field.

Diffraction analysis of fibrous materials is too important for this effort to be postponed or evaded. Many linear polymer systems inherently are incapable of forming crystals of any great lateral extent. Indeed, many of the properties of gel-forming polysaccharides (for example) arise specifically from molecular bundling that is not very extensive. These and other repetitious polymers also are often quasi-cylindrical so that even the limited lateral order in their fibres is not periodic. The structures of all of these less-than-fully-crystalline systems are capable of being analysed quantitatively by X-ray diffraction methods, some more easily than others and to different levels of resolution. In all these circumstances it seems needlessly limiting for

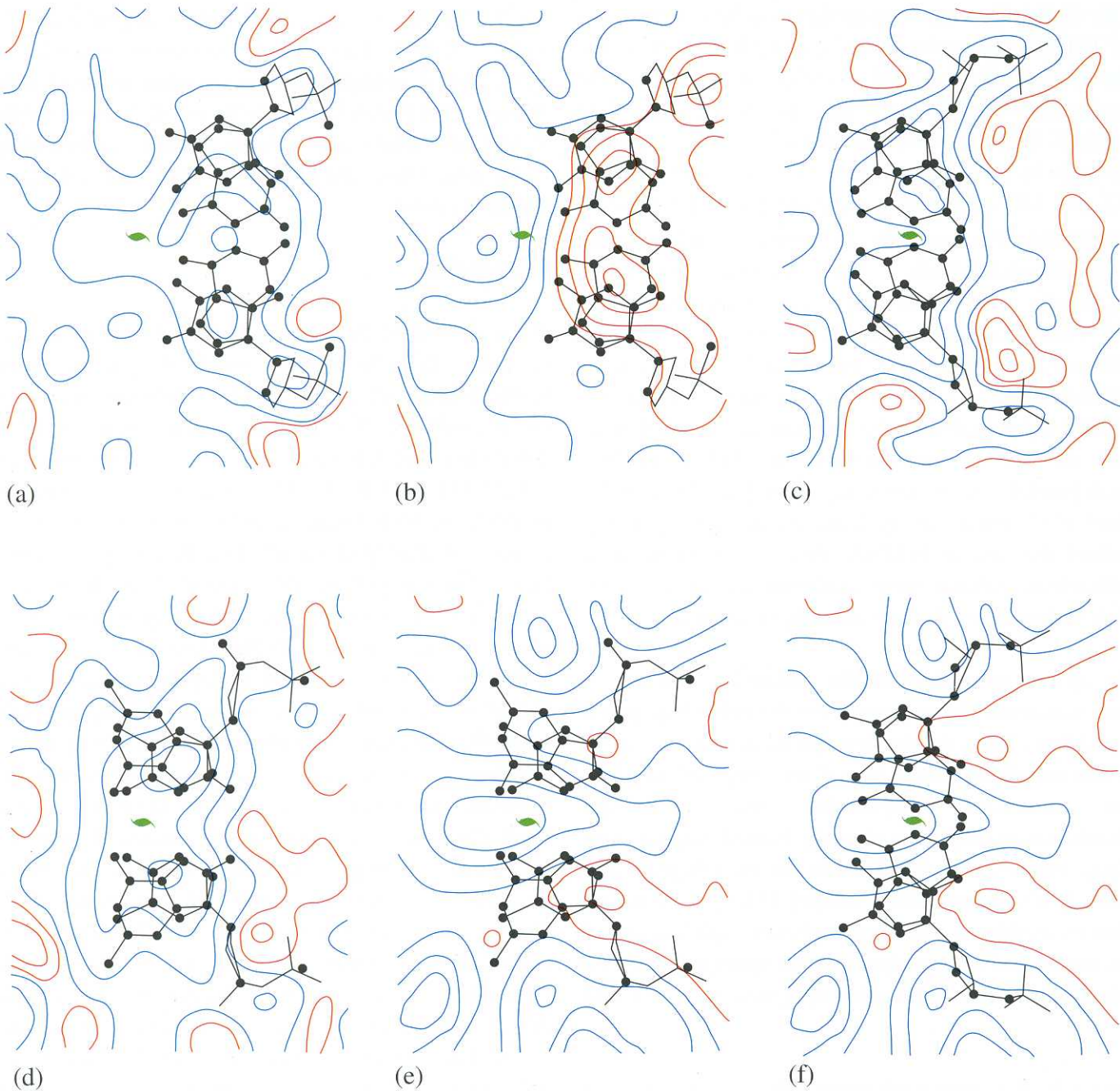


**Figure 5:** (a) The electron density distribution in the plane of an (average) Watson-Crick base pair obtained with observed amplitudes and phases derived from the original Crick and Watson coordinates for DNA. The image is not only of poor resolution but discordant with the model. (b) The difference map shows that the major deficiency of the model is the position of the base-pairs in the negative (red contoured) region rather than astride the helix axis. (c) When the molecular morphology had been changed by Wilkins' refinements a new electron density synthesis with better phases shows a more concordant fit between model and experiment. (d) A biased electron density distribution calculated [14] using phases from a DNA model with Hoogsteen pairs. (e) The corresponding difference map shows that density is needed in places that cannot be accessed without changing the type of base-pairing as illustrated in (f) where a refined Watson-Crick-type model is superposed on the same difference map.

progressive structurists to concentrate only on systems that crystallize and even more suspect to focus only on surrogate oligomers that also happen to crystallize. To do so must result in the selection of a very small subset of structures for detailed analysis and the postponement for decades of the discovery of other structures, thereby distorting the global view. If

we take only the fibre structures illustrated in this article as examples we can highlight the predicament: DNA-RNA hybrid duplexes with non-identical anti-parallel chains have been observed only in fibres; the same is true of the ladder-like DNA duplex complexed with an intercalated drug; collagen tripleplexes were discovered to be dimorphic

in fibres fourteen years before this was confirmed in a crystal; the behaviours of starch, cellulose, as well as connective tissue and other gel-forming polysaccharides have been rationalized exclusively from fibre diffraction studies; the structures of DNA and RNA single, double, triple and quadruple helices were defined from fibre analyses up to a quarter of a century before analogous structures were disclosed in single crystals.

Fibre diffraction analysis has many past achievements to be proud of and many future triumphs to anticipate.

## References

- [1] Wang, A.H.-J., Quigley, G.J., Kolpak, F.J., Crawford, J.L., van Broom, J.H., van der Marel, G. and Rich, A., *Nature* (1979) **281**, 680.
- [2] Arnott, S., Chandrasekaran, R., Birdsall, D.L., Leslie, A.G.W. and Ratliff, R.L., *Nature* (1980) **287**, 561.
- [3] Dickerson, R.E., *Meth. Enzymol.* (1992) **211**, 67.
- [4] Arnott, S., Chandrasekaran, R., Millane, R.P. and Park, H.-S., *J. Mol. Biol* (1986), **188**, 631.
- [5] Rich, A. and Crick, F.H.C., *J. Mol. Biol* (1961) **3**, 483.
- [6] Fraser, R.D.B., MacRae, T.P. and Suzuki, E., *J. Mol. Biol* (1979) **129**, 463.
- [7] Okuyama, K., Arnott, S., Takayanagi, M. and Kakudo, M., *J. Mol. Biol*. (1981) **152**, 427.
- [8] Bella, J., Eaton, M., Brodsky, B. and Berman, H.M., *Science* (1994) **266**, 75.
- [9] Chandrasekaran, R., in *Adv. in Carbohydrate Chemistry and Biochemistry* (1997) **52**, 311.
- [10] Balazs, E.A., *Fed. Proc* (1966) **25**, 1817.
- [11] Arnott, S. and Wonacott, A.J., *J. Mol. Biol* (1966) **21**, 371.
- [12] Arnott, S., Mitra, A.K. and Ragunathan, *J. Mol. Biol* (1983) **169**, 861.
- [13] Crick, F.H.C. and Watson, J.D., *Proc. R. Soc. (London) Ser. A* (1954) **223**, 80.
- [14] Arnott, S. in *Bull. Inst. Phys. and Phys. Soc* (1964), 169-178.
- [15] Arnott, S., Wilkins, M.H.F., Hamilton, L.D. and Langridge R., *J. Mol. Biol* (1965) **27**, 391.
- [16] Arnott, S., in *Oxford Handbook of Nucleic Acid Structure* (1998), 1-36.

## X-Ray Studies on Biological Fibres

A. Miller, J.P. Orgel and T.J. Wess

University of Stirling

The most important scientific paper of the second half of the twentieth century was a report of X-ray fibre diffraction studies on DNA. Biological fibres have well developed crystallinity in the direction of the fibre axis, but are not so well ordered in the directions normal to the fibre axis. This simple one-dimensional order meant that fibres allowed the first recognition of the secondary structure of proteins - the alpha helix, beta sheet, coiled-coil alpha helix and collagen helix - as well as the double helix of DNA, long before X-ray crystallography yielded the full three-dimensional structures of biological macromolecules and complexes. In addition X-ray fibre diffraction studies gave information about the molecular packing in the native biological fibres of muscle, tendons and the cytoskeleton and it is this window into structural molecular biology which is the subject of this note.

Advances in the technology of X-ray fibre diffraction have always been the basis of its value. Small angle cameras with good resolution between the undeflected beam and the scattered beam closest to it, good reciprocal spatial resolution throughout the scattered pattern, intense X-ray sources of high spectral brilliance and efficient and effective X-ray detectors have all played their part. So we will start by discussing some aspects of synchrotron radiation which are undergoing developments which will be relevant to fibre work - as well as to macromolecular crystallography - in the near future. We then summarise our recent work on the molecular packing of Type I collagen in tendons and comment on recently published claims about features in the X-ray diffraction patterns from the alpha-keratin of hair and their relationship to breast cancer.

## Synchrotron Radiation

Third generation synchrotron sources such as the ESRF at Grenoble introduced the feature of flexibility of insertion devices which could be custom designed for specific scientific applications. In second generation synchrotrons the flexibility lay mainly in the design of the beam lines. Hence at ESRF, once the machine energy was decided as 6

GeV and the emittance of the electron beam set as  $7 \times 10^{-9}$  nm.rad, the task remained to survey the proposals of the scientist users and to build a set of beam-lines on Insertion Devices (IDs) tailored within technically feasible limits for defined areas of science. A balance was struck between beam-lines which would allow a high volume of new science to be done and other beam-lines which served smaller groups of scientists working at extremes of technology such as in high X-ray energy, high pressure studies or recondite techniques such as Mossbauer scattering.

Since the ESRF was founded in 1986 and opened in 1993 as planned, there have been many advances in machine design allowing lower emittance electron beams and improvements in ID design which will affect the choice of energy of the new generation of synchrotron sources and in particular allow lower energy (and thus cheaper) machines to produce X-rays of high brilliance in the energy range up to 20KeV. The main parameter in IDs which can be lowered is the inter-magnet gap across the electron beam. When ESRF started this was set prudently at a minimum of 20 mm. Now ESRF can run with a gap of 8 mm. The lower gap means that with a fixed electron beam energy in the machine and fixed magnetic field in the ID the energy of the emitted X-rays is higher than with a wider gap. At a meeting held in Daresbury in May 1999 (Chair - M.W. Poole) there were reports of experiences with smaller gaps at synchrotron sources world wide. It was concluded that to achieve gaps of lower than 5 mm it was necessary to have the magnets of the ID *in vacuo* and then gaps of 2 mm could be countenanced. However, operation *in vacuo* brings additional technical problems and risks. A. Ropert concluded that *in vacuo* was necessary for a gap less than 5 mm and Marcouille working with calculations done for SOLEIL concluded that 25 KeV X-rays can be produced with a 1.5 m long *in vacuo* device with a 4 mm gap from a 2.5 GeV machine. Another factor emerging from recent experience of building undulators is that high harmonics - around the 11th - can be used with tolerable loss in brilliance. These considerations are central in discussions about machine energy, design of IDs and of beam-lines for fibre diffraction at the planned UK-Wellcome-French synchrotron.

### Molecular Packing in Collagen

We have produced a model-independent solution to

the phase problem for a native biological fibre, Type I collagen in tendon, using Multiple Isomorphous Addition (Orgel, Wess and Miller, 2000). This technique has been used previously to produce an electron density projection on to the fibre axis (Bradshaw *et al.* 1989) where the first 52 meridional orders of diffraction in the X-ray fibre pattern were used.

Using synchrotron radiation at Daresbury Laboratory, UK (Beamlines 7.2 and 2.1) and at the European Synchrotron Radiation Facility, Grenoble, France (Beamline ID2) we have recorded over 140 meridional orders of diffraction. Of these, 124 orders from native tendons and tendons stained isomorphously with gold chloride and potassium iodide have been utilised to produce the electron density profile in Figure 1. The resolution of this electron density projection is more than two times higher than that produced previously.

The new electron density map to 0.54 nm resolution reveals that the collagen molecule *in vivo* is 4.54 D long, where each staggered segment (D) is 66.7 nm and corresponds to 234.2 amino acids. It also shows that the C-terminal telopeptide is in a folded conformation and the N-terminal telopeptide is axially contracted compared with the conformation in the collagen triple helix.

However, the key findings of this new high resolution study pertain to the intermolecular crosslinks which are essential to maintain the structural integrity of the collagen fibrils in native healthy tissue (Eyre *et al.*, 1984). The telopeptides are those formed by amino acid sequences at the end of the molecule which do not have the regular Gly-X-Y feature and so cannot coil into the collagen triple helical conformation.

There are 25 amino acids in the alpha 1 C-terminal chain and our electron density projection presents strong evidence that there is a hairpin turn at proline 13 and glutamine 14. This would bring tyrosine residue 24 into axial alignment with tyrosine 4 and bring lysine 17 into a favourable position to form a lysine-hydroxylysine crosslink with hydroxylysine 87 thus helping to stabilise the fibril structure (Figure 2).

This study provides for the first time model-independent information about the all important intermolecular crosslinks.

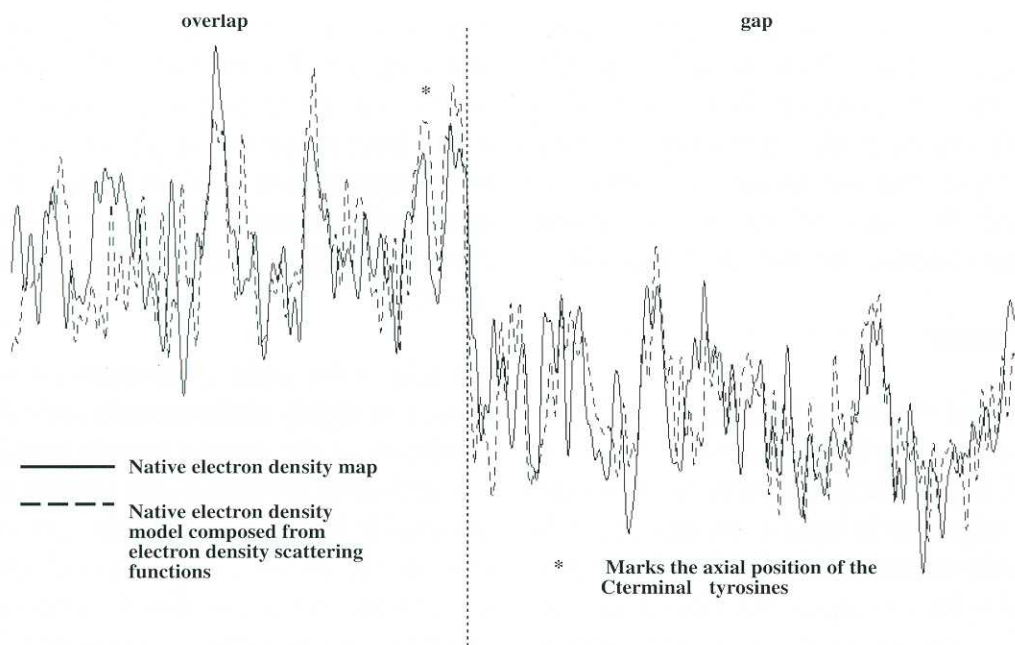


**Figure 1:** 1-Dimensional Electron density profile of type I collagen. The resolution of the electron density projection (or 1D electron density map) is 0.54 nm. Overlaid is an electron density model composed from residue scattering factors and the amino acid sequence. The residue spacing in the model was constant, the N-telopeptide contracted by 85%, and the C-telopeptide was folded at residues 13 and 14.

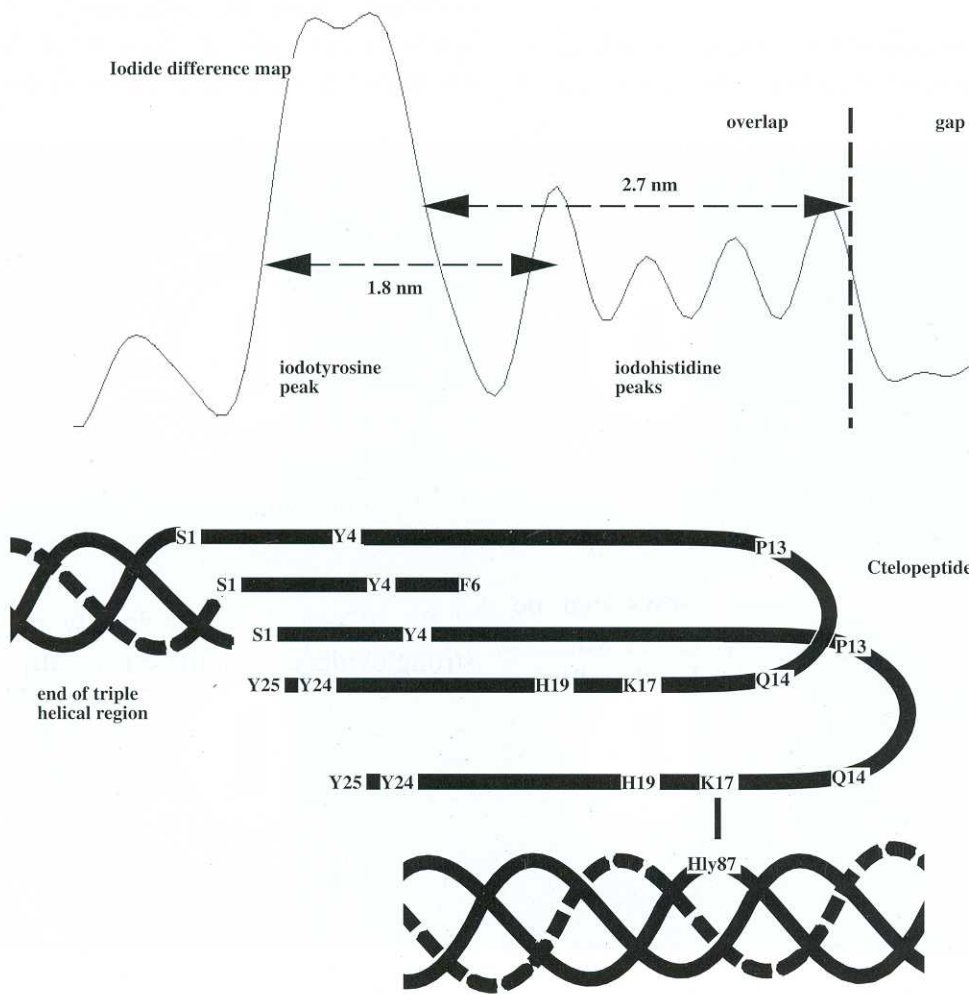


**Figure 2:** Conformation of the C-telopeptide restricted by heavy atom positions. An expanded view of the C-terminal telopeptide region shows a conformation that corresponds well with the difference density data.

We are now carrying out a similar project to obtain a model-independent three-dimensional electron density distribution of collagen in native tendon. Obviously the resolution in the electron density map will be anisotropic, but we expect to locate the telopeptides and the sites of the intermolecular crosslinks and to visualise the molecular packing.

## Keratin and Cancer

In an article entitled “Using hair to screen for breast cancer” James *et al.* (1999) reported that the occurrence in X-ray diffraction patterns from female human hair of rings due to lipid scattering could be correlated with the occurrence in the female subjects of a gene linked to breast cancer. Needless to say this report attracted widespread comment in the media. We wish to criticise the conclusion drawn by James *et al.* on several grounds. First the number of samples used in the study was far too small to justify the conclusion. Secondly, there was no discussion of other factors such as the effect on hair of state of health of the subjects, washing detergents, anti-cancer drug therapy etc.

However, the most important criticism is that there was no reference to earlier work on the occurrence of

lipid rings in the X-ray diffraction patterns from alpha keratin (Fraser *et al.* 1963). This is particularly significant since Fraser *et al.* presented evidence for a mechanism for the origin of the lipid rings. The best interpretation that can be put on this is that the apparently dramatic findings of James *et al.* were published in ignorance of a highly relevant previous study.

Keratin is the main component of human hair and occurs in highly differentiated cells dedicated to the synthesis of the protein keratin within the cells. As keratinisation progresses the keratin fills the cell and eventually kills it. The hair and skin on the surface of humans are mostly composed of dead cells. Fraser *et al.* carried out a combined X-ray diffraction and electron microscopy examination of hair as it develops from the follicle just under the skin to the fully keratinised tissue. They found that in the early stages of keratinisation there were no lipid rings in the X-ray diffraction patterns from hair at that point. As keratinisation progressed away from the follicle the lipid rings appeared. Electron microscopy showed that the appearance of these rings could be correlated with the appearance of crystallites of lipids in the cells as they were deformed by the development of keratin fibres (Fraser *et al.*, 1963).

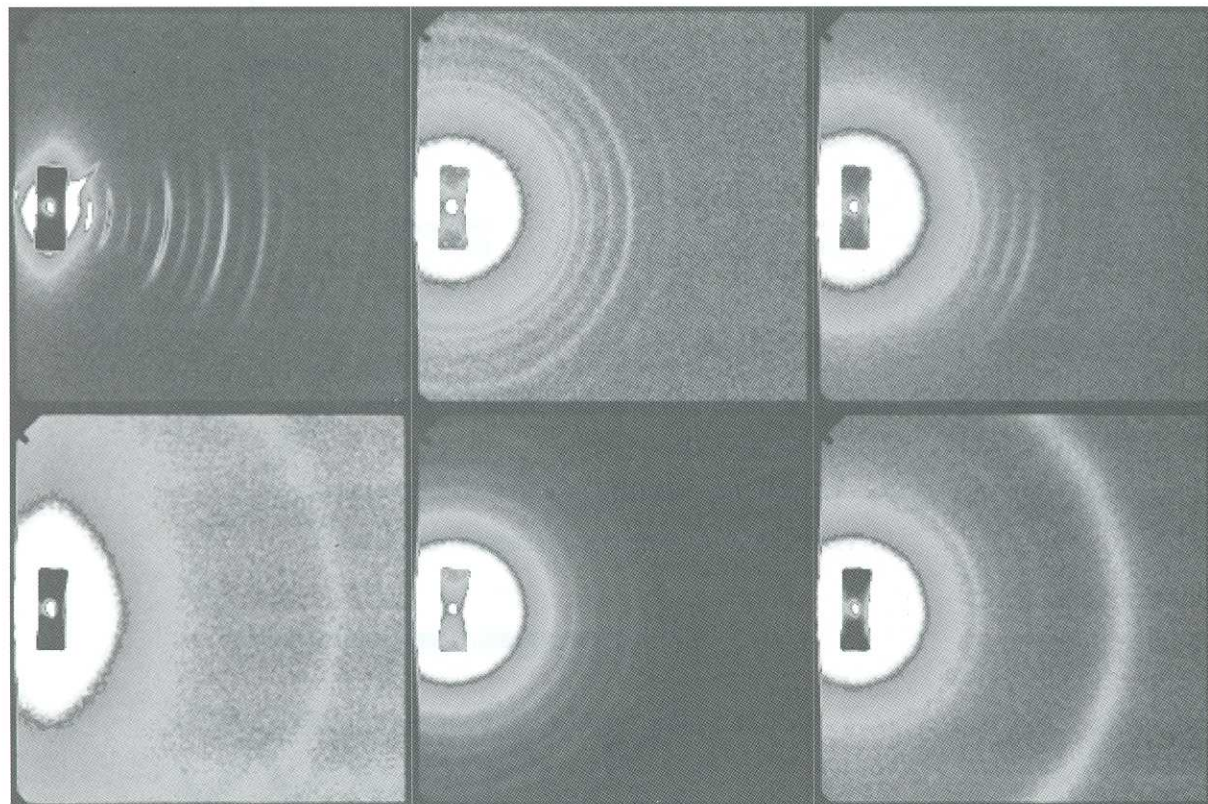


**Figure 3:** X-ray diffraction image of dry collagen samples containing diffuse isotropic diffraction ring from lipids. The samples are historic parchment sample from the 17th century provided by the Danish National Archive. Unpublished results indicate that lipid crystallisation is related to ageing of the parchment samples. The lipid ring corresponds to a periodicity of 4.5nm. Data were collected using a 6 metre camera on beamline 2.1 of the Daresbury synchrotron.

The lipid crystallites in the electron micrographs showed bands spaced some 4.7 nm apart and this spacing corresponded with that observed in the lipid rings in the X-ray diffraction patterns. The crystallites seemed to be formed by rearrangement of the membranes of the cell mitochondria.

On the basis of what is in the scientific literature at present there is no reason to believe that the variation in appearance of lipid rings in X-ray diffraction patterns from hair is not due to the degree of keratinisation in the hair cells and is unrelated to cancer. Indeed, Wilk, James and Amemiya (1995) reported that "oil" is an integral component of all samples of human scalp hair.

It is worth pointing out that X-ray diffraction patterns from other biological fibres such as collagen often contain rings that index on the lipid spacing (Figure 3).

An alternative explanation for the presence of the isotropic diffraction ring is possible due to its close proximity with the 4.5 nm equatorial diffraction peak. The 4.5 nm reflection corresponds to the cylindrical transform of an  $\alpha$ -helical bundle. It is possible that keratin samples exhibiting diffuse scatter contain microfibrils that are randomly orientated and have a low packing density. These would exhibit negligible intermolecular interference and produce arcs of diffuse scatter that would roughly correspond to those observed by James *et al.* Samples containing disordered arrays of microfibrils suggest that the biogenesis of the hair was disrupted in some way. Perhaps it is possible that radiation and chemotherapy would cause such disruption.

## References

- [1] Fraser, R.D.B., MacRae, T.P., Rogers, G.E. and Filshie, B.K., *J. Mol. Biol.* (1963) **7**, 90-91.
- [2] James, V., Kearsley, J., Irving, T., Amemiya, Y. and Cookson, D., *Nature* (1999) **398**, 33-34.
- [3] Wilk, K.E., James, V.J. and Amemiya, Y., *Biochim. Biophys. Acta.* (1995) **1245**, 392-396.
- [4] Eyre, D.R., Paz, M.A. and Gallop, P. M., *Ann. Rev. Biochem.* (1984) **53**, 717-748.
- [5] Bradshaw, J.P., Miller, A. and Wess, T.J., *J. Mol. Biol.* (1989) **205**, 685-694.
- [6] Orgel, J.P., Wess, T. J. and Miller, A., *Structure* (2000) **8**, 134-141.

## Unravelling Starch Granule Structure with Small Angle Scattering

A.M. Donald, P. A. Perry and T.A. Waigh

Cavendish Laboratory, Madingley Road, Cambridge CB3 OHE, UK

## Introduction

Starch is a natural source of polymers of huge commercial importance both for food and industrial use (as in paper-coatings). As knowledge of starch biochemistry improves, as does the ability of plant scientists to produce novel starches (not necessarily, but possibly, via genetic modification routes), it is important to be able to understand the impact of such changes on structure and subsequent processing. In order to explore the hierarchical internal structure of the native granule, and how it breaks down during processing ('cooking'), small angle scattering of both neutrons and X-rays have been used in a complementary approach.

The native starch granule contains two main polysaccharides, amylopectin and amylose. Amylopectin is highly branched and is the component which crystallises. It does so via double helix formation of the side chain branches which then aggregate to form the crystals. Amylose, on the other hand, is an essentially linear polysaccharide. The proportions of these two polysaccharides, and the molecular weights of the chains (which are always very high, running to many millions in the case of amylopectin) are species-dependent. However, in wild-type species, there is usually approximately 70% amylopectin and 30% amylose. Most starches contain minor amounts of other components including lipids and proteins, but they will not be further discussed here.

## Experimental Methods

Various different commercially available starches have been used. Each starch has been made up as a slurry at 40-45 w/w% in the appropriate solvent (water, which may have included D<sub>2</sub>O for SANS experiments, or glycerol). The starch slurry was sealed in a cell which was made of aluminium for SAXS experiments, and quartz for SANS. Experiments were carried out on beamline 8.2 at the

SRS, Daresbury UK and LOQ at the ISIS Spallation Source, Rutherford Appleton Laboratory, UK. Further details can be found in [1-3].

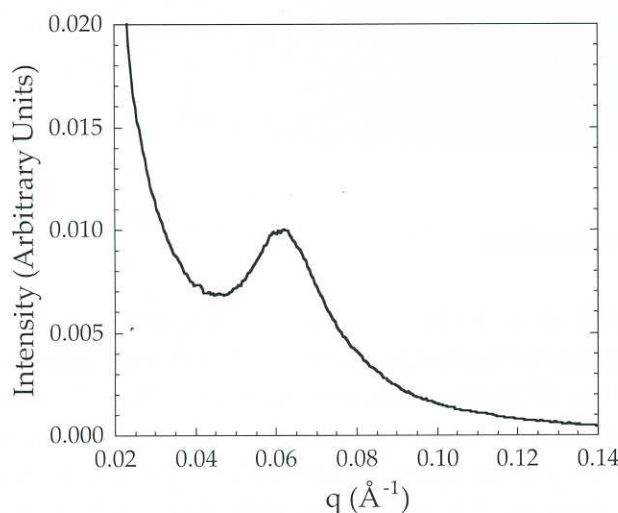


**Figure 1:** SAXS curve of hydrated maize starch using a 40 w/w% starch solution in water.

## Results

It has long been known that the native granule structure is characterised by a strong peak in the low angle region (Figure 1), corresponding to an approximately 9nm spacing. Recent work in Cambridge has enabled a detailed model of the generic structure of starch granules to be built up, as shown in Figure 2. This basic model shows 3 different types of region. These are alternating amorphous and semicrystalline growth rings, with the latter themselves comprising alternating lamellae of crystalline and amorphous regions. The alternating rings of higher and lower order have also been identified from  $\alpha$ -amylase digestion and the name “growth rings” stems from the belief that they

arise from diurnal fluctuations in the way the starch is laid down [4-6]. Having obtained a general picture of the hierarchical make-up of the granule, it is important now to understand how different conditions and source materials affect the organisation within the various regions.

The first key piece of information is that the strong peak corresponding to the lamellar repeat of ~9nm, is essentially the same independent of species [7]. However, it appears that there are systematic changes in the proportion of this repeat (which is crystalline) as the ratio of amylopectin to amylose changes through a family of mutants [8]. Figure 3 illustrates this in terms of electron density differences for the 3 different regions, in aqueous slurries of the maize family (where the three mutants shown all occur naturally). The relative heights of the lines in these diagrams reflect the relative electron densities, so that crystalline regions always have the highest value; they are the most electron dense. Whether the amorphous lamellae have higher or lower electron densities than the amorphous growth rings is species/mutant dependent.

However, it is not always easy to extract absolute values from SAXS patterns, so that these graphs only show relative values. Using SANS provides us with a new variable, since by altering the amount of  $D_2O$  in the aqueous phase of the sample, variation in the contrast between different regions can be obtained for the same starch sample. Full details of how contrast variation can be used to quantify the amount of water in different regions of the starch granule can be found elsewhere [2,3,9]. Unfortunately, the neutron scattering is quite weak, so that the statistics tend not to be so good as for SAXS data. Nevertheless it is possible to draw some very

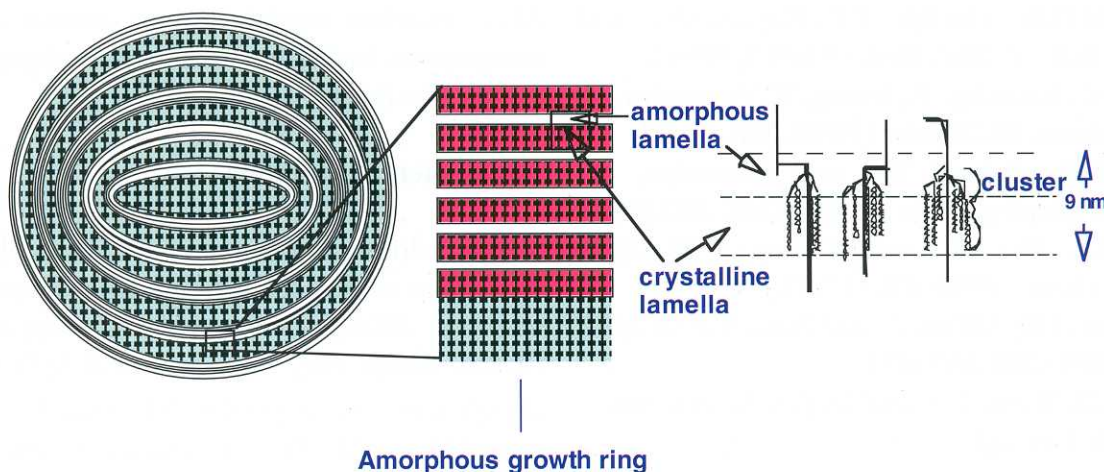


**Figure 2:** Model of the starch granule used to fit SAXS and SANS data (after [1]).

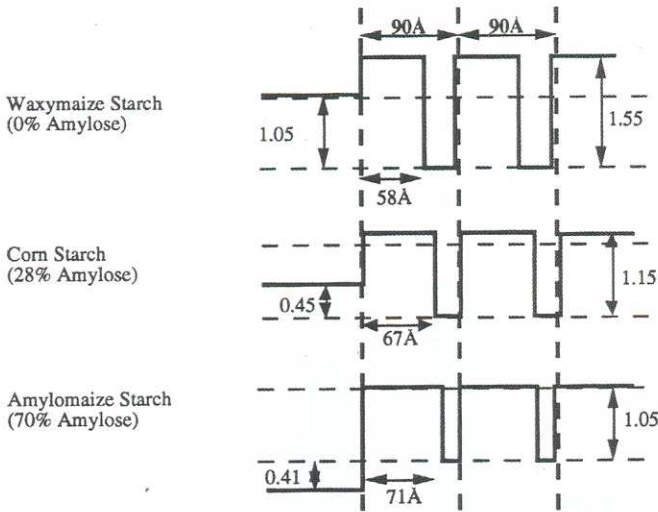


**Figure 3:** Electron density profiles for 3 cultivars in the maize family (data from [8]). The vertical dashed lines show the essentially constant 9nm repeat for the family. The repeat consists of alternating crystalline (high electron density) and amorphous (low) lamellae within the semicrystalline growth ring. The third region is the amorphous growth ring.

interesting conclusions regarding the distribution of water.

Firstly, it is known from wide angle scattering that starches which exhibit the so-called A polymorph, such as cereals, contain far less water as an integral part of the crystalline unit cell than starches exhibiting the B polymorph (mainly tubers such as

potato) [10]. Analysis of the SANS data demonstrates this difference too (Figure 4). As might be expected, there is far more water within both types of amorphous region than within the crystals, as can also be seen from Figure 4. If the concentration of starch in the aqueous suspension is increased into the so-called ‘limiting water’ regime [11], which is known to have a significant impact on the subsequent breakdown of the granule during gelatinisation (such as cooking), then the impact of this external water concentration also is revealed by small changes in the internal water content, as shown in Figure 5.

This finding suggests that how the granule breaks down when heat is applied may be driven, at least in part, by the internal water content. Indeed, the whole granule structure may be significantly altered if the water level drops too low. Returning to the use of SAXS, Figure 6 shows what happens to the scattering when dehydration takes place: the strong peak arising from the 9nm periodicity completely disappears. Simultaneously, the peak (at the edge of the wide angle regime) corresponding to the 100 interhelix spacing also disappears. This second observation means that the traditional explanation for the loss of the 9nm peak upon dehydration as ‘loss of contrast’ is not correct. Rather there must be some significant structural changes which remove correlations both between helices and the longer range correlations between crystalline lamellae.

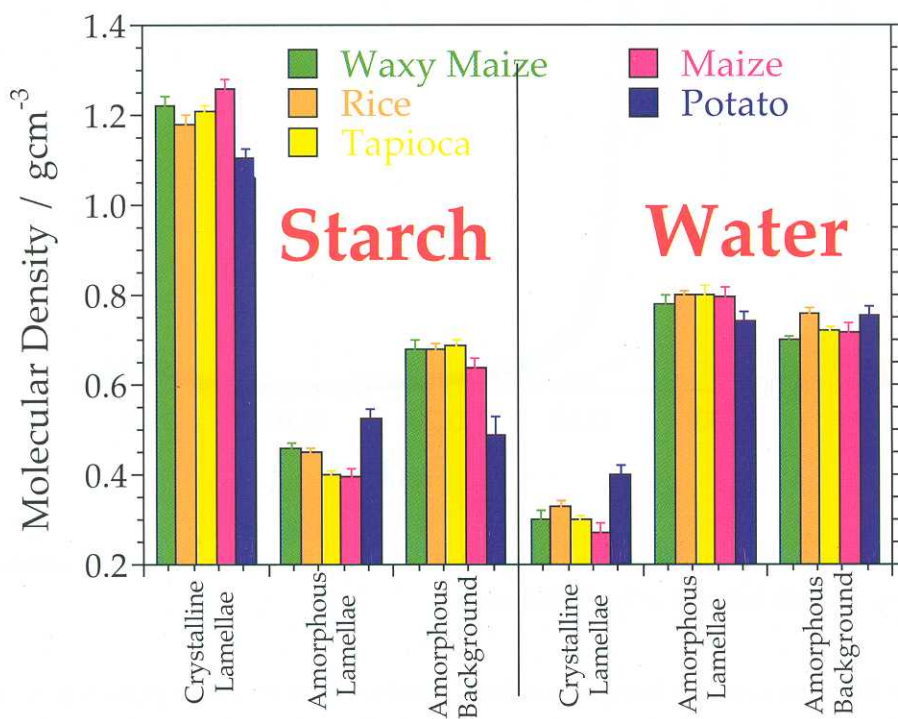


**Figure 4:** The molecular densities of the starch and water within the three regions of the starch granules of waxy maize, maize, rice and tapioca – all A type starches – and potato, a B type starch.

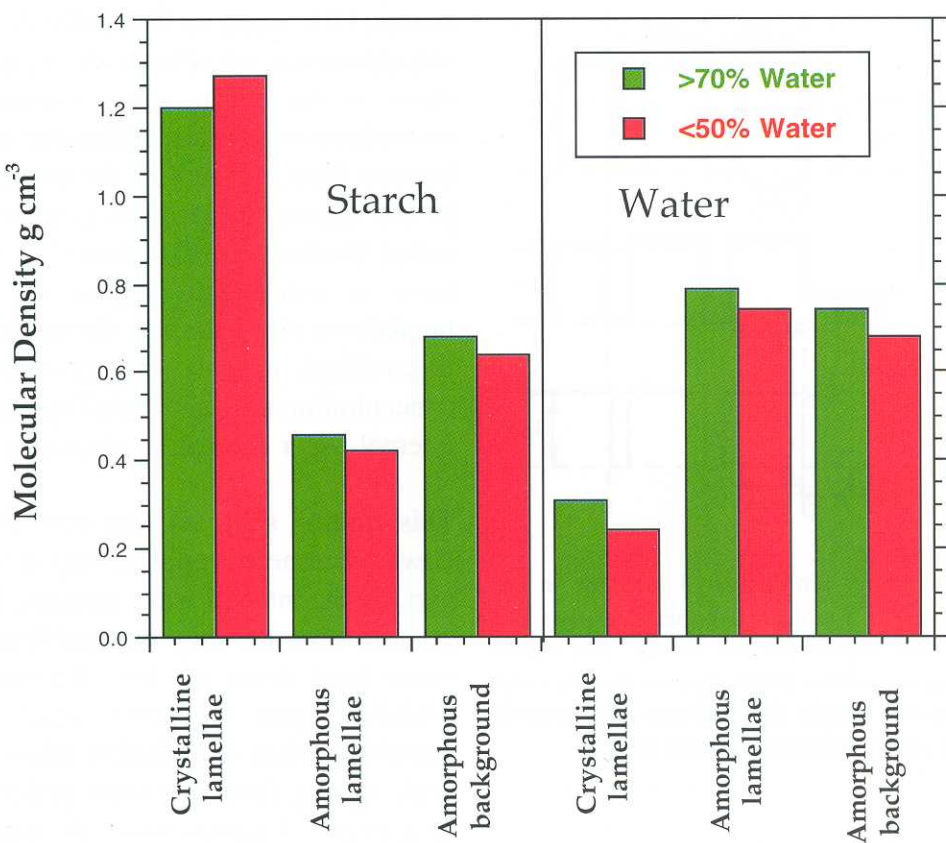


**Figure 5:** The molecular densities of starch and water within the three regions of waxy maize starch granules at two different levels of bulk water.

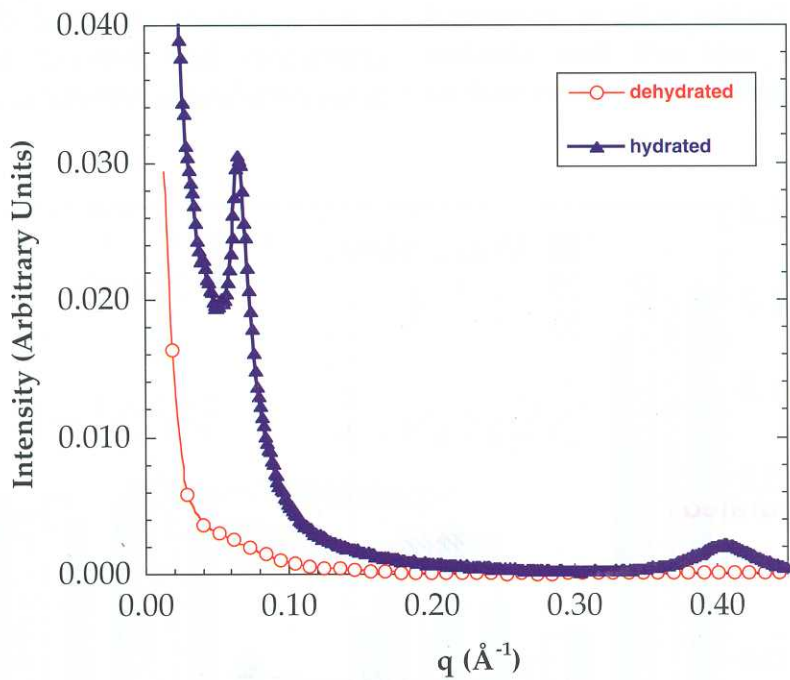


**Figure 6:** SAXS data for potato when hydrated and dehydrated. The peak at high  $q$  in the hydrated case corresponds to the interhelix (100) reflection, normally detected in the WAXS range.

The interpretation of these structural changes can be found by reconsidering the nature of the packing in the alternating lamellae. By considering these lamellae as corresponding to smectic layers, with the

double helices corresponding to the mesogens of a side chain liquid crystalline polymer, it is possible to see what may be happening upon dehydration (Figure 7). In the hydrated (plasticised) state, Figure

7(b), the side chains are sufficiently decoupled from the backbone to permit good alignment of the double helices to form smectic layers with long range correlations and good lateral packing of the helices. As dehydration occurs, the ‘flexible spacer’ in the vicinity of the amylopectin branch points becomes less mobile, and it is no longer possible to maintain this degree of order (Figure 7(a)). The structure now more closely resembles a nematic. The side chains are still in layers, but with reduced correlations both between and within the layers.

In non-aqueous solvents, similar effects can be seen. When a granule is initially placed in pure glycerol (a plasticiser frequently used for starch when processed as a thermoplastic [12,13]), the SAXS curves show no 9nm peak. Upon storage at room temperature, this 9nm peak can be seen to grow. Accompanying this structural change, an endotherm can also be detected in DSC traces, and this endotherm moves to lower temperatures with storage time until, after around 24 hours, it can no longer be detected. These two findings indicate that glycerol ingress is quite slow (the molecule is after all significantly larger than

water), but as it does enter the granule and plasticises the amylopectin branchpoints, self-assembly can occur of the semicrystalline lamellae into smectic layers. Since this process requires the intake of thermal energy, an endotherm is detected. Figure 8 indicates schematically how the organisation within the semicrystalline lamellae changes with uptake of the solvent.

Finally, these changes in room temperature organisation must be reflected in the way the granule breaks down during the process known as gelatinisation. Using simultaneous WAXS and SAXS it is possible to follow the changes which occur as the granules are heated in water at both the short and the longer lengthscale in real time. These data, coupled with limited information from SANS (for which the low intensity of scattering means that for most samples it is difficult to obtain real time data) show that water enters the amorphous growth rings first. At this point the granules start to swell – visible optically – but initially there is little change in the semicrystalline lamellae. As heating continues, more water enters the granule and amylose leaches

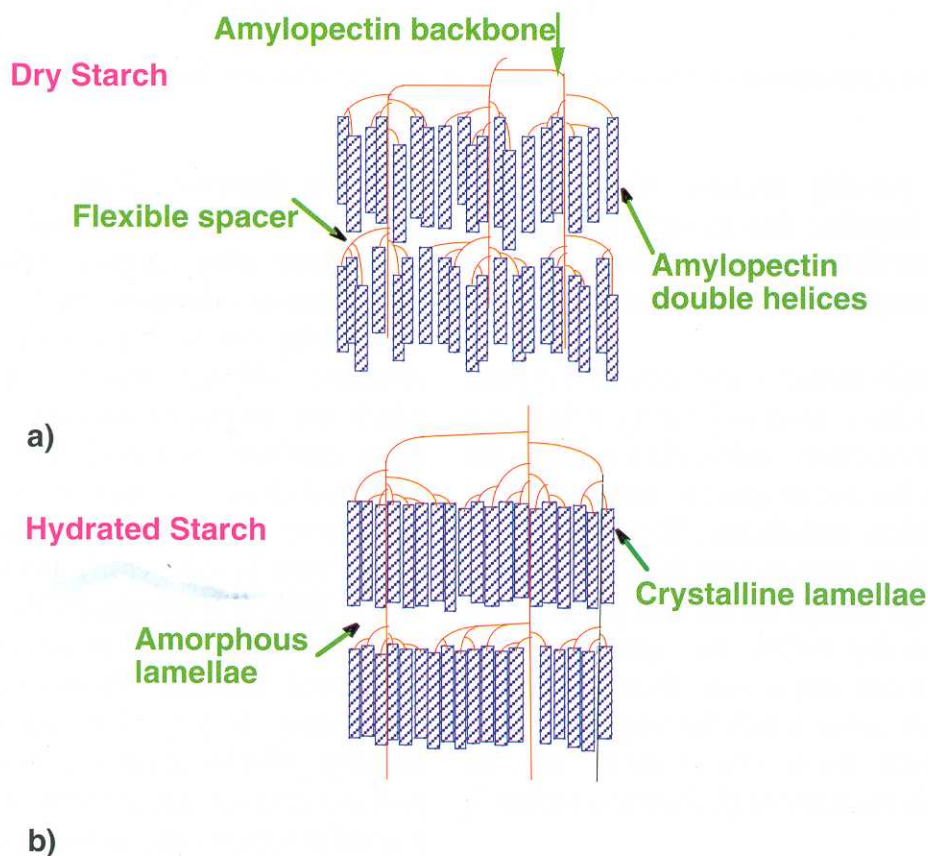


**Figure 7:** Schematic representation of the amylopectin viewed as a side chain liquid crystalline polymer. The double helices represent the mesogens, and are shown as blocks. In the dehydrated state the organisation is essentially nematic, but in layers (Figure 7(a)). When hydrated the double helices can align better and the structure becomes a smectic (Figure 7(b)).

## Increasing Solvation & Plasticisation

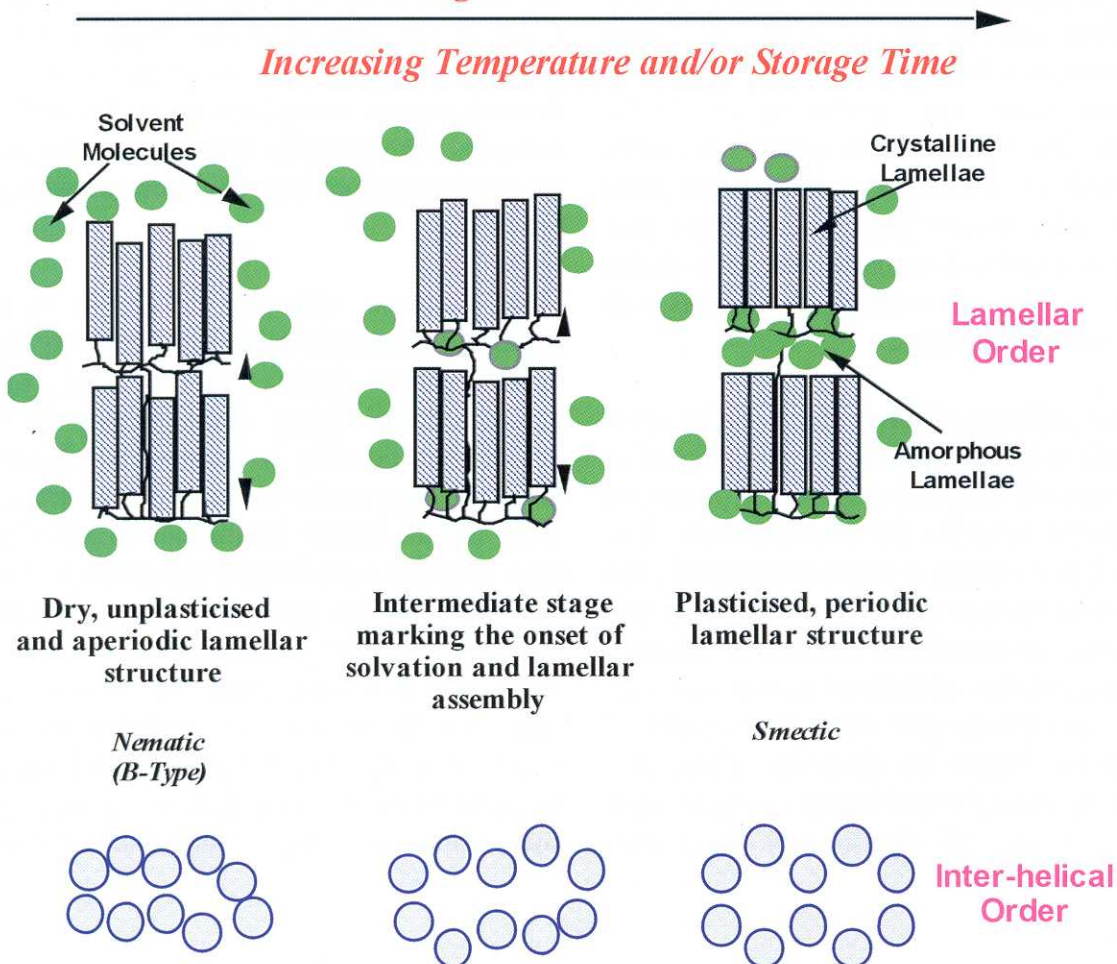


**Figure 8:** Schematic representation of how solvation affects the ordering within the lamellae for B-type starch.

out. Eventually, possibly because of the stresses imposed on the lamellae due to the swelling, the crystalline regions themselves are destroyed. This corresponds to completion of gelatinisation.

However, this simple picture is insufficient to explain the fine detail of what is observed. Firstly, it has been shown that the crystallinity index, derived from the WAXS data [14], has not dropped to zero by the end of the gelatinisation endotherm. Secondly, if the heating is only taken partway into the gelatinisation endotherm, but high enough for the 9nm peak to have dropped in intensity before the temperature is dropped back to room temperature, there is a certain critical temperature below which the long range order can reform. Both these observations can be rationalised within the framework shown in Figure 7.

As heating starts to affect the organisation of the crystalline lamellae, the helices move out of register, and the structure resembles that of the nematic state in Figure 7(a). By this point, the crystallinity index

starts to decrease. However some intrahelical structure - which can still contribute to the crystallinity index - appears to be left by the end of the gelatinisation endotherm. Thus all the long range crystallinity may be lost, and the thermal transition is complete, although there is residual local order which the particular measure of the crystallinity index continues to record. The second observation described above, also indicates that the movement of the double helix 'mesogen' blocks in and out of register may be quite easily accomplished. It appears that at modest temperatures the packing may shift from the regular lamellar (smectic) structure to the disordered nematic. However, as long as the temperature is kept low enough that the basic building blocks remain constant, then cooling permits rapid reordering to the original structure. The particular temperature at which this ability is lost is species dependent. A comparison of maize and waxy maize (in which there is no amylose) suggests that the amylose in wild-type maize may start to migrate into the lamellae during heating, and essentially

interpose between the helices. The effect of this is to impede the re-formation of the lamellar structure upon cooling. Thus the critical temperature is lower for maize than for waxy maize, for which the lack of amylose removes this specific problem.

## Conclusions

Scattering techniques are proving very powerful in discovering how the internal order within starch granules is affected by external parameters. Using a combination of SAXS and SANS, as well as WAXS data, it is becoming possible to understand the factors that determine how the granular structure breaks down during processing. With the advent of new starch cultivars and mutants it is increasingly important to rationalise the factors which are important in controlling structure, so that optimisation of the utilisation of starch can be achieved. Scattering techniques provide one approach to providing this information.

## References

- [1] Jenkins, P.J., Cameron, R.E., Donald, A.M., Bras, W., Derbyshire, G.E., Mant, G.R. and Ryan, A.J., *J. Poly. Sci. Phys. Ed.* (1994) **32**, 1579-83.
- [2] Jenkins, P.J. and Donald, A.M., *Polymer* (1996) **37**, 5559-68.
- [3] Jenkins, P.J. and Donald, A.M., *Carb. Res.* (1998) **308**, 133-147.
- [4] Buttrose, M.S., *Journal of Ultrastructure Research* (1960) **4**, 231-257.
- [5] Buttrose, M.J., *Cell Biol.* (1962) **14**, 159-167.
- [6] Buttrose, M.S., *Stärke* (1963) **15**, 85-92.
- [7] Jenkins, P.J., Cameron, R.E. and Donald, A.M., *Stärke* (1993) **45**, 417-20.
- [8] Jenkins, P.J. and Donald, A.M., *Int. J. Biol. Macromols* (1995) **17**, 315-21.
- [9] Waigh, T.A., Jenkins, P.J. and Donald, A.M., *Far. Disc.* (1996) **103**, 325-337.
- [10] Imbert, A., Buleon, A., Tran, V. and Perez, S., *Starch* (1991) **43**, 375-84.
- [11] Donovan, J., *Biopolymers* (1979) **18**, 263-75.
- [12] Tomka, I., in *Thermoplastic starch* (Ed. I. Tomka) **627-637** (Plenum, New York, 1991).
- [13] Simmons, S., Weigand, C.E., Albalak, R.J., Armstrong, R.C. and Thomas, E.L., *Fundamentals of Biodegradable Materials and Packaging* (1992).
- [14] Wakelin, J.H., Virgil, H.S. and Crystal, E., *J. Appl. Phys.* (1959) **30**, 1654-1662.

## Structure of Block Copolymer Solutions

T. P. Lodge and K. J. Hanley

Department of Chemistry and Department of Chemical Engineering and Materials Science, University of Minnesota, 207 Pleasant Street SE, Minneapolis, MN 55455-0431

*The addition of solvent to a diblock copolymer melt affects a variety of order-order transitions between different phases, as well as the order-to-disorder transition. The sequence of phases with dilution and/or heating may be anticipated qualitatively on the basis of diagonal trajectories across the melt phase map, but there are a variety of novel features as well. At sufficiently dilute concentrations, suspensions of micelles are observed, and the critical micelle temperature in dilute solution is similar to the order disorder temperature at intermediate concentrations.*

## Introduction

Block copolymers are a class of macromolecular surfactants that self-assemble into a variety of microstructures [1, 2]. In many applications, notably in adhesive formulations, block copolymers are diluted with low molecular weight additives to modify relevant mechanical properties such as tack. However, the ordered phase symmetry may also depend on diluent concentration and temperature. We are pursuing a systematic experimental assessment of the phase behavior of block copolymer solutions, utilizing a series of solvents of varying selectivity for the two blocks. The experimental results are also supported by self-consistent mean-field calculations of free energies. In this work we describe the effects of varying solvent selectivity on the phase behavior of a particular styrene-isoprene diblock copolymer.

## Experimental

The styrene-isoprene (SI) diblock copolymer was synthesized by standard living anionic polymerization protocols, as previously described [3]. It has block molecular weights of 11,000 (S) and 21,000 (I), with an overall polydispersity of 1.04. The composition and molecular weight were established by NMR and size exclusion chromatography with light scattering detection, respectively. The solvents bis(2-ethylhexyl) phthalate (DOP), di-n-butyl phthalate (DBP), and di-

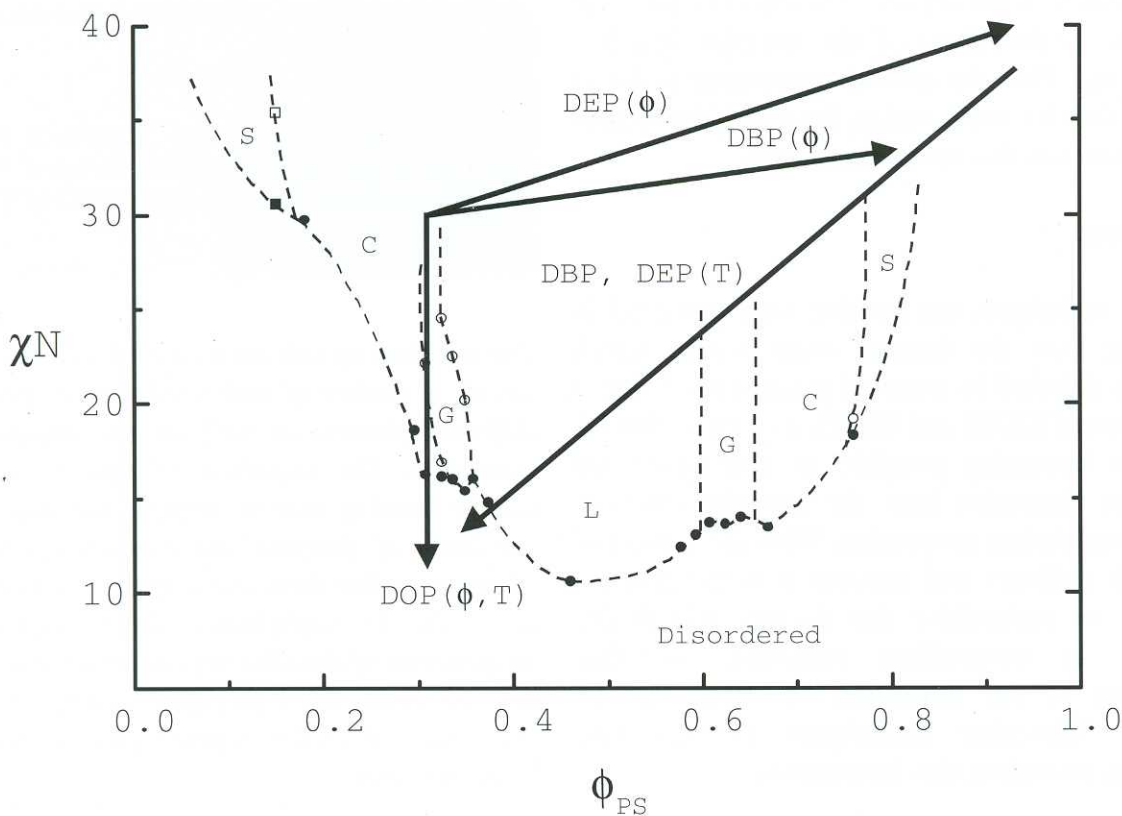


**Figure 1:** Phase map for styrene-isoprene diblock copolymers in the melt. The solid arrows indicate the qualitative effects of adding neutral (DOP) and slightly selective (DBP, DEP) solvents as a function of volume fraction ( $\phi$ ) and also of heating (T).

ethyl phthalate (DEP) were obtained from Aldrich and purified by neutralizing with 5% aqueous sodium bicarbonate, rinsing with distilled water, drying over calcium chloride, and vacuum distilling prior to use. Solutions were prepared gravimetrically, with methylene chloride as a co-solvent. The co-solvent was stripped off under vacuum, and polymer volume fractions,  $\phi$ , calculated assuming additivity of volumes and densities of 0.981, 1.043, and 1.18 g/mL for DOP, DBP, and DEP, respectively.

The phase behavior was determined by a combination of small-angle X-ray scattering (SAXS), static birefringence, and rheology. SAXS measurements were taken on the University of Minnesota beamline, using  $\text{Cu K}_\alpha$  radiation ( $\lambda = 1.54 \text{ \AA}$ ) from a Rigaku RU-200BVH rotating anode and Franks mirror optics. Scattered X-rays were collected on an area detector (Siemens), corrected for detector response, and azimuthally averaged to give intensity  $I$  (arbitrary units) versus scattering wavevector  $q$ . Static birefringence measurements were made as previously described [3], utilizing a 5 mW HeNe laser, an initial polarizer, an orthogonal analyzer after the sample, and a photodiode detector.

For isotropic samples (either disordered or cubic phases) the transmitted depolarized intensity is essentially zero, but the lamellar and cylindrical phases depolarize the light to a finite extent. Thus SAXS is necessary to establish the symmetry of a given phase, but birefringence is a rapid way to locate thermotropic transitions. Rheology is also a standard means to locate transitions, as the low frequency shear elastic modulus is very sensitive to the state of order [4]. Measurements were taken on a Rheometric Scientific DSR in the parallel plate geometry. In all cases, transition temperatures located by two or more techniques were in quantitative agreement.

## Results and Discussion

The phase behavior of diblock copolymer melts is reasonably well understood [1]. The experimental phase map for SI diblock copolymers is shown in Figure 1, and is largely consistent with other measurements on this system [5, 6]. Furthermore, the essential features (*i.e.*, identity and location of the particular ordered phases) is captured by self-consistent mean-field (SCMF) theory [7, 8]. The vertical axis is the product of the degree of

polymerization,  $N$ , and the styrene-isoprene interaction parameter,  $\chi$ . The latter represents the heat of mixing per monomer unit, normalized by  $kT$ . The major morphologies are lamellae (L), cylinders of the minor component packed on a hexagonal lattice (C), and spherical micelles packed on a bcc lattice (S). The choice of structure is determined primarily by the volume fraction of one block,  $\phi$ . A bicontinuous cubic phase, the gyroid (G, space group Ia  $\bar{3}d$ ), is found for compositions between L and C, but only near the order-disorder transition (ODT) (A perforated layer (PL) or modulated layer (ML) phase is often seen near the G phase, but this is now understood as a metastable intermediate that will ultimately anneal into G [9]).

The qualitative effects of adding a solvent to a block copolymer melt are also illustrated by the arrows in Figure 1. If a solvent is neutral *i.e.* it is an equally good solvent for both blocks, the addition of solvent is analogous to increasing temperature. The dilution of contacts between monomers reduces the effective  $\chi$  parameter. On the other hand, if a very selective solvent is employed, it will preferentially segregate into that microdomain. The resulting phases can be anticipated to some extent simply by computing a renormalized  $\phi$ , assuming complete partitioning of the diluent. However, the  $\chi$  parameter between the solvent and the unfavorable block often exceeds that between the two monomers, and thus the arrow indicates that the effective degree of segregation,  $\chi N$ , also increases with added solvent. Thus solvents with differing degrees of selectivity will move the system to lesser or greater degrees of segregation. Upon heating, another interesting situation develops. The solvent will generally become less selective, and therefore redistribute itself more uniformly between the microdomains, as  $T$  increases. Consequently, in contrast to the neutral solvent case, there will be a diagonal trajectory back across the phase map. A rich variety of lyotropic and thermotropic order-order transitions (OOT) should thus be accessible.

These qualitative features are all evident in measurements on SI(11-21) in DOP, DBP, and DEP, as shown in Figures 2(a), (b) and (c). In the melt, SI(11-21) exhibits an OOT from G→C upon heating, and the ODT at 238°C. At low T the PS glass transition intervenes and prevents further study of equilibrium phases. As DOP is a neutral solvent, both the ODT and OOT move to lower T as the solvent concentration increases, and no new structures are observed. However, one can see that the window of

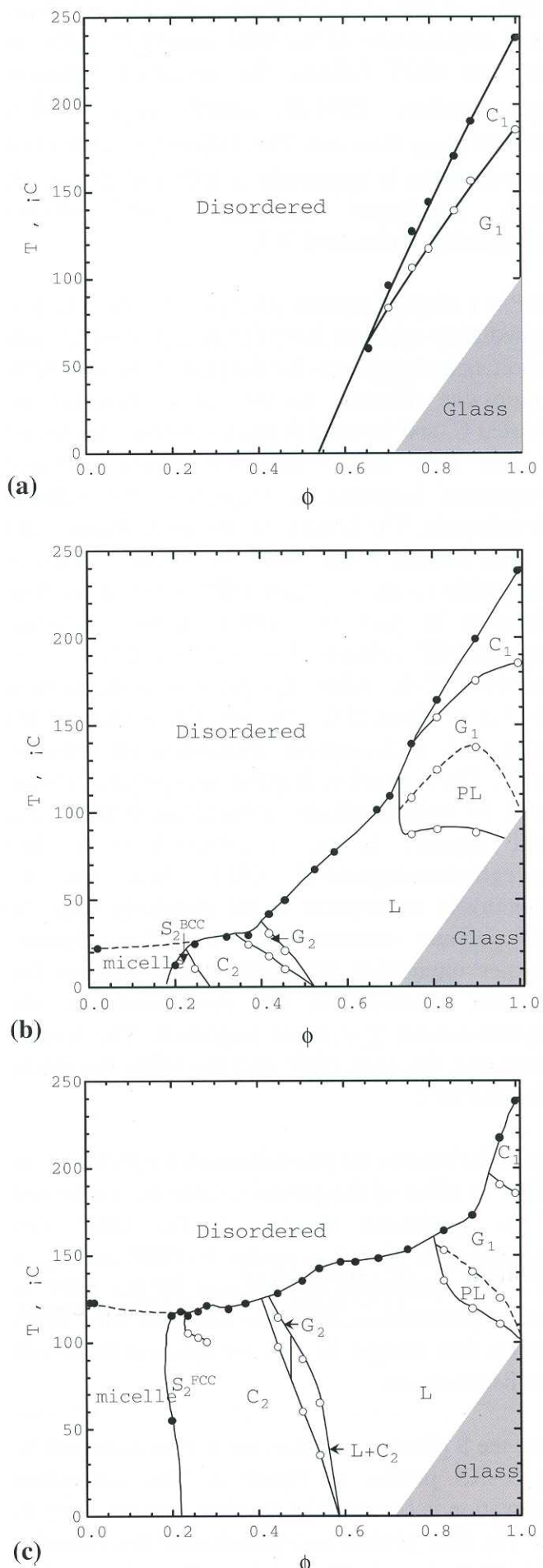


**Figure 2:** Phase diagrams for a styrene-isoprene diblock copolymer with block molecular weights of 11,000 and 21,000 dissolved in (a) DOP, (b) DBP, and (c) DEP.

C phase shrinks and disappears with dilution. Thus, the T dependences of the ODT and OOT differ. In fact, the OOT follows the so-called “dilution approximation” [10-12], namely  $\chi_{OOT} \sim \phi^{-1}$ , whereas  $\chi_{ODT}$  does not. This failure of the dilution approximation is apparently a universal feature in block copolymer solutions, and remains incompletely understood [13].

DBP is a slightly styrene selective solvent, and it is immediately apparent from Figure 2(b) that this has important consequences for the phase behavior. With progressive dilution, regions of L, inverted G, inverted C, and inverted S phases appear. “Inverted” in this case means that the major polymer component, isoprene, is located in the smaller microdomain. The boundaries between phases tend to slant toward lower  $\phi$  as T increases. This is attributable to the fact that DBP is becoming less selective; in fact the critical temperature for isoprene/DBP solutions has been estimated to be near 90°C [14]. When the polymer concentration falls below about 20%, the micelles no longer fill space, and a disordered suspension of micelles results. These micelles disperse into polymer chains above the critical micelle temperature (CMT). The CMT appears to be a continuation of the concentration-dependent ODT. This can be qualitatively understood in the following way. At high polymer concentrations, it is the polymer-polymer interaction parameter that dominates the behavior, whereas for low concentrations, the polymer-solvent  $\chi$  is more important. The former determines the melt ODT and the latter the dilute solution CMT.

Figure 2(c) shows the phase diagram for SI(11-21) in DEP. The effect of the greater selectivity is reflected in the significant increase in the ODT. The progression of phases is similar to DBP, and again the CMT determines the location of the ODT at lower concentrations. However, there are some novel features that emerge for this solvent, and these will now be discussed.

First, the S phase is now fcc, not bcc, as indicated by the SAXS pattern in Figure 3. This interesting observation is consistent with some previous reports [15, 16]. One general interpretation of this behavior relies on the range of the intermicellar potential. For micelles with short corona blocks, the interaction is short-ranged, and just like hard spheres, the micelles select the close-packed fcc lattice. In the melt, it is

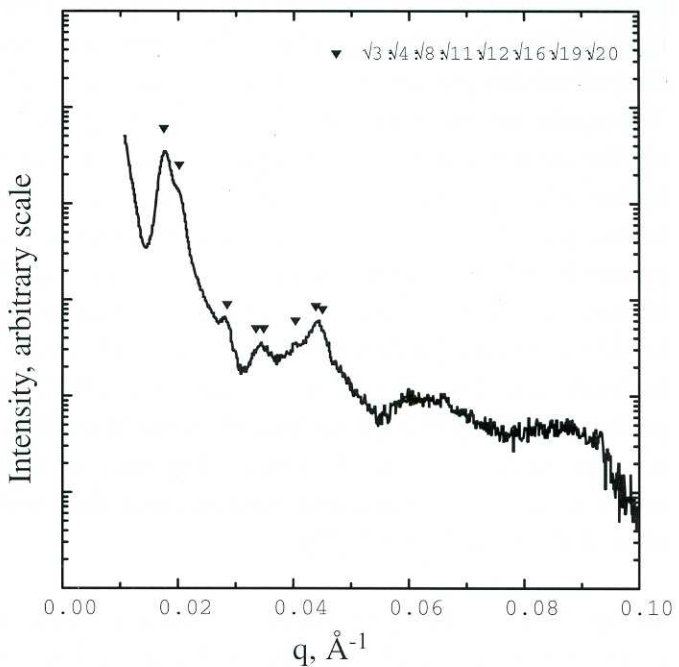


**Figure 3:** SAXS pattern for the  $\phi = 0.26$  solution in DEP showing the allowed reflections for an fcc phase.

the major block that forms the corona, imparting a long-range interaction that favors the bcc arrangement. However, this argument is not sufficient to fully explain the results here, because in DBP at the same concentration, the spheres adopt the bcc lattice, whereas the coronal conformation should be the same.

Second, there is a re-entrant ordered phase for the solution with  $\phi = 0.2$ , namely below about 50°C the solution is a disordered suspension of micelles, but upon heating it transforms to an fcc lattice, before melting at the ODT near 120°C. This may be ascribed to swelling of the micelles. At low temperature the micelles are just on the brink of reaching the effective volume fraction necessary to order on a lattice. Upon heating, the solvent becomes less repelled by the isoprene cores, and the micelles swell. This is sufficient to induce the ordering transition, but as temperature increases the solvent dissolves the isoprene core and the solution melts.

Third, near  $\phi = 0.55$ , there is a wide region of coexisting L and C. The experimental signature of this is shown in Figure 4. The observation of a region of coexistence is not surprising in itself, given that it is a two-component system; in general one expects coexistence regions along each phase boundary. However, in all the other cases this region is

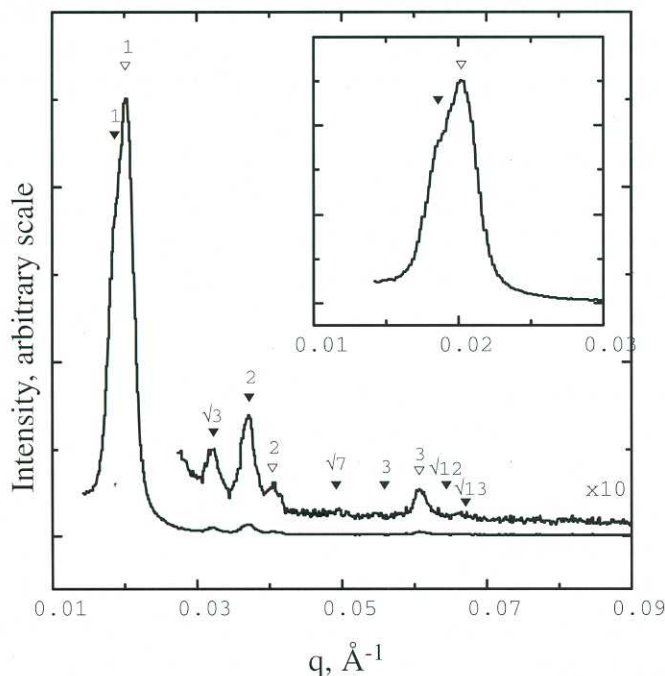


**Figure 4:** SAXS pattern for the  $\phi = 0.54$  solution in DEP showing the coexisting lamellar and hexagonal phases.

extremely narrow, probably on the order of 1°C wide, whereas in this case the interval is as much as 40°C. This is presumably attributable to the subtle balance of chain stretching, packing frustration, and conformational asymmetry that ultimately determines the precise location of the phase boundary.

## Summary

The addition of solvents of varying selectivity to a styrene-isoprene diblock copolymer reveals a rich array of lyotropic and thermotropic transitions. The sequence of ordered phases may be approximately anticipated by the concept of diagonal trajectories on the melt phase map, but important distinctions are also exposed.

## Acknowledgements

This work was supported in part by the National Science Foundation through award DMR-9528481.

## References

- [1] Bates, F.S. and Fredrickson, G.H., *Annu. Rev. Phys. Chem.* (1990) **41**, 525.
- [2] Hamley, I.W., in *The Physics of Block Copolymers* (Oxford University Press, Oxford, 1998).
- [3] Hanley, K.J. and Lodge, T.P., *J. Polym. Sci., Polym. Phys. Ed.* (1998) **36**, 3101.
- [4] Fredrickson, G.H. and Bates, F.S., *Annu. Rev. Mater. Sci.* (1996) **26**, 503.
- [5] Khandpur, A.K., Förster, S., Bates, F.S. et al., *Macromolecules* (1995) **25**, 8796.
- [6] Winey, K.I., Gobran, D.A., Xu, Z. et al., *Macromolecules* (1994) **27**, 2392.
- [7] Matsen, M.W. and Bates, F.S., *Macromolecules* (1996) **29**, 1091.
- [8] Matsen, M.W., *Phys. Rev. Lett.* (1995) **74**, 4225.
- [9] Hajduk, D.A., Takenouchi, H., Hillmyer, M.A. et al., *Macromolecules* (1997) **30**, 3788.
- [10] Hong, K.M. and Noolandi, J., *Macromolecules* (1983) **16**, 1083.
- [11] Fredrickson, G.H. and Leibler, L., *Macromolecules* (1989) **22**, 1238.
- [12] Olvera de la Cruz, M., *J. Chem. Phys.* (1989) **90**, 1995.
- [13] Lodge, T.P., Pan, C., Jin, X. et al., *J. Polym. Sci., Polym. Phys. Ed.* (1995) **33**, 2289.
- [14] Lodge, T.P., Xu, X., Ryu, C.Y. et al., *Macromolecules* (1996) **29**, 5955.
- [15] McConnell, G.A. and Gast, A.P., *Macromolecules* (1997) **30**, 435.
- [16] Hamley, I.W., Pople, J.A. and Diat, O., *Colloid Polym. Sci.* (1998) **276**, 446.